International Journal of Biological Macromolecules 257 (2024) 128464

Contents lists available at ScienceDirect

International Journal of Biological Macromolecules

journal homepage: www.elsevier.com/locate/ijbiomac

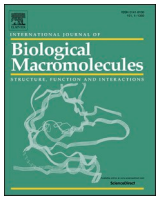

Proteome landscape and interactome of voltage-gated potassium channel 1.6 (Kv1.6) of the murine ophthalmic artery and neuroretina

Natarajan Perumal [a,1], Hajime Yurugi [b,1], Katrin Dahm [b], Krishnaraj Rajalingam [b], Franz H. Grus [a], Norbert Pfeiffer [a], Caroline Manicam [a,*]

[a] Department of Ophthalmology, University Medical Centre of the Johannes Gutenberg University Mainz, Mainz, Germany
[b] Cell Biology Unit, University Medical Centre of the Johannes Gutenberg University Mainz, Germany

ARTICLE INFO

Keywords:
Affinity purification-mass spectrometry
Ophthalmic artery
Proteomics
Retina
Voltage-gated potassium channel

ABSTRACT

The voltage-gated potassium channel 1.6 (Kv1.6) plays a vital role in ocular neurovascular beds and exerts its modulatory functions *via* interaction with other proteins. However, the interactome and their potential roles remain unknown. Here, the global proteome landscape of the ophthalmic artery (OA) and neuroretina was mapped, followed by the determination of Kv1.6 interactome and validation of its functionality and cellular localization. Microfluorimetric analysis of intracellular [K^+] and Western blot validated the native functionality and cellular expression of the recombinant Kv1.6 channel protein. A total of 54, 9 and 28 Kv1.6-interacting proteins were identified in the mouse OA and, retina of mouse and rat, respectively. The Kv1.6-protein partners in the OA, namely actin cytoplasmic 2, alpha-2-macroglobulin and apolipoprotein A-I, were implicated in the maintenance of blood vessel integrity by regulating integrin-mediated adhesion to extracellular matrix and Ca^{2+} flux. Many retinal protein interactors, particularly the ADP/ATP translocase 2 and cytoskeleton protein tubulin, were involved in endoplasmic reticulum stress response and cell viability. Three common interactors were found in all samples comprising heat shock cognate 71 kDa protein, Ig heavy constant gamma 1 and Kv1.6 channel. This foremost in-depth investigation enriched and identified the elusive Kv1.6 channel and, elucidated its complex interactome.

1. Introduction

The voltage-gated potassium ion (Kv) channels constitute one of the largest ion channel superfamilies of pore-forming six transmembrane proteins found in both excitable and non-excitable cell types [1,2]. This complex channel family plays crucial roles in a myriad physiological processes owing to their remarkable ion selectivity function as well as their influence on the initiation and propagation of membrane potential [3–5]. A large majority of the Kv channels are found in the mammalian brain, particularly in neurons and glial cells, which corresponds to the functionality of these channels in the regulation of action potentials, synaptic transmission and plasticity [6–9]. This potassium ion channel subtype is also an important component of the vascular smooth muscle cells that exerts diverse modulatory actions ranging from dictating the vasomotor tone of arteries by maintaining the potassium ion homeostasis to exquisite controlling of the membrane potential [10–15]. Perturbations in the expression patterns, impaired activity and mutations lead to abnormal functionality of the Kv channels, which are often manifested as a vast number of channelopathies such as neurological diseases, cancer, cardiovascular and autoimmune disorders [1,16–18]. Hence, several Kv channels, particularly the members of the Kv1 family, have emerged as attractive therapeutic targets for a diverse disease conditions [19–21].

Most channels belonging to the Kv1 or mammalian *Shaker* family (Kv1.1-Kv1.6) include mainly slowly activating and inactivating delayed rectifier channels with widespread distribution in an array of tissues, including the eye [22,23]. Our previous study identified the Kv1.6, a delayed rectifier voltage-gated potassium channel, as one of the functionally important channels that mediates the vasodilator responses in a major retrobulbar blood vessel, the ophthalmic artery [12]. Interestingly, this channel subtype has also been shown to have specific distribution in the retina [24,25]. Both latter studies explored the

* Corresponding author at: Department of Ophthalmology, University Medical Centre of the Johannes Gutenberg University Mainz, Langenbeckstr. 1, 55131 Mainz, Germany.
E-mail address: caroline.manicam@unimedizin-mainz.de (C. Manicam).
[1] Shared first authorship.

https://doi.org/10.1016/j.ijbiomac.2023.128464
Received 29 August 2023; Received in revised form 14 November 2023; Accepted 25 November 2023
Available online 2 December 2023

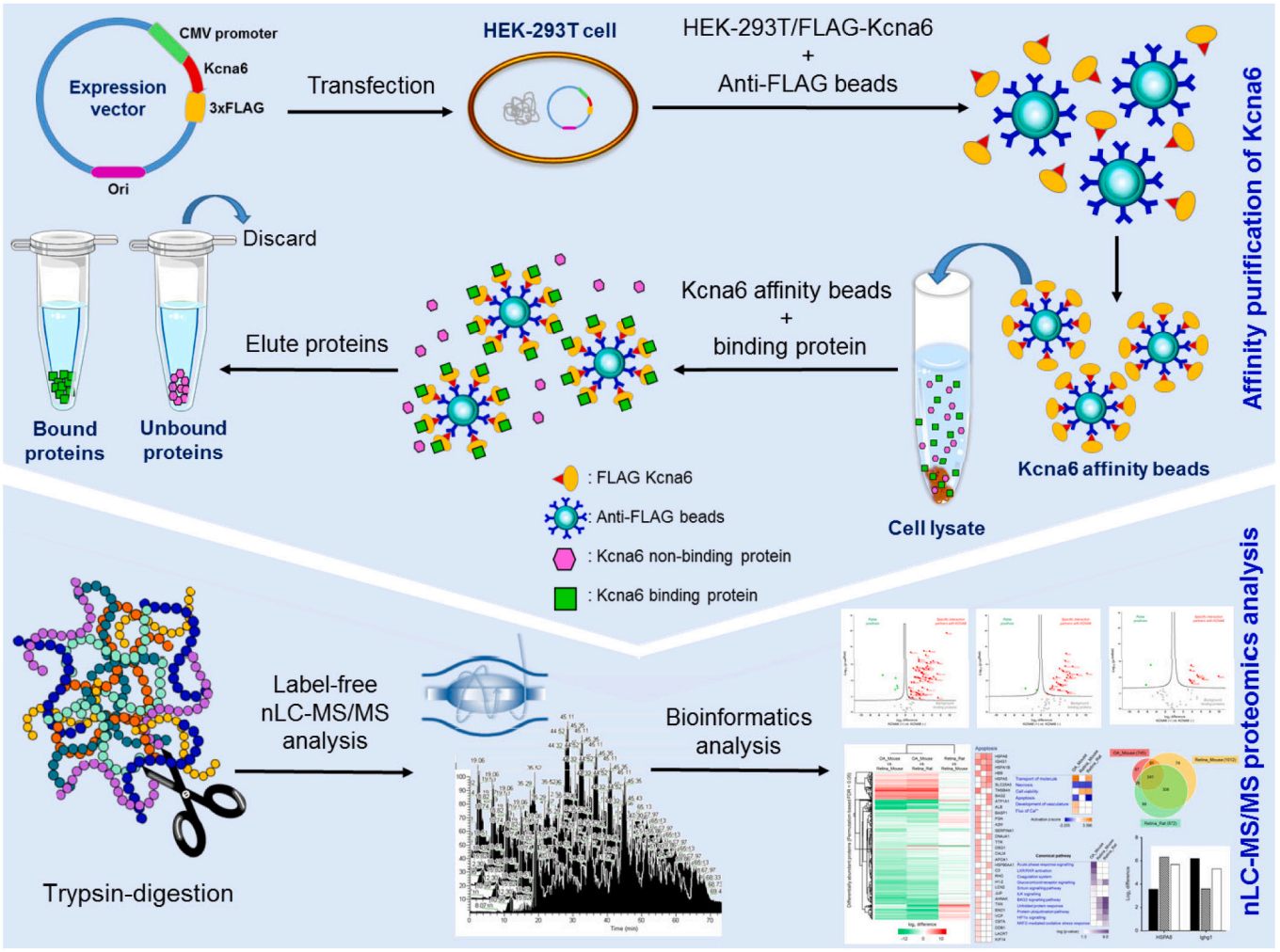

Fig. 1. The schematic outline of the experimental workflow employed to characterize the Kv1.6 channel-protein interactors using cell transfection and affinity purification mass spectrometry (AP-MS)

Voltage-gated potassium channel Kv1.6 cDNA was amplified for cloning into p3xFLAG-CMV-14 expression vector and transfected into HEK-293 T cells. Affinity purification of bait protein and the interacting prey proteins was conducted following cell lysis employing the anti-FLAG M2 affinity beads mixed with ophthalmic artery and retinal tissue lysates. Eluted proteins were tryptic-digested and analysed in the MS. The acquired data were subjected to bioinformatics analyses employing different tools to characterize the interactome.

differential expression and effects of different trophic factors on the Kv1.6 channel, respectively, in the rat retina at different postnatal stages, and reported that this channel is expressed predominantly in the retinal ganglion cells, with accentuated distribution in other retinal cell layers and types. This is not surprising since the retina is an extension of the central nervous system with striking anatomical and functional similarities to the brain [26,27]. In line of neurological studies, a recent study by Salpietro et al. provided exciting novel evidence that the *Kcna6* gene, which encodes for the Kv1.6 channel, is associated with epilepsy with neurodevelopmental disorder [28]. Another study by Gunasekaran et al. has previously shown that the cerebrospinal fluid of patients suffering from a fatal neurodegenerative disease, Amyotrophic Lateral Sclerosis (ALS), decreased the expression of the Kv1.6 channel in motor neurons, which may lead to neuronal degeneration [29].

The Kv channels are often components of larger protein networks as it is known that proteins perform their functions *via* interaction with other proteins, which dictate the ultimate modulatory actions of the channels [30]. Remarkably, the members of this ion family also exhibit roles that are largely independent of their K^+-conducting properties, which influence the biophysical features and pharmacological properties of these ion channels, owing to their versatile interaction with a diverse auxiliary signalling proteins [2,7,21]. These protein-protein interaction (PPI) modalities are essential components that ensure proper intercellular communications as well as the modulation of other signal transduction pathways involved in the maintenance of cellular homeostasis. Therefore, the identification of molecular partners of the Kv channels has emerged as an important avenue to gain a broader insight into the functions of the interacting proteins. Recent innovations in mass spectrometry (MS)-based proteomic approaches and bioinformatics have enabled the elucidation of protein signalling networks in different sample types. However, the isolation, accurate identification and annotation of Kv channels and their PPIs in complex samples such as tissues and blood vessels remain a challenge owing to poor detection sensitivity of low abundant proteins [31]. Likewise, albeit the identification and confirmation of the cellular localization, as well as determination of specific vaso-functionality of the Kv1.6 channel in the ophthalmic artery in our previous study [12], we have not been able to identify this channel subtype in our MS-based proteomics analyses to date [32,33]. In recent years, affinity purification combined with mass spectrometry (AP-MS) has emerged as a preeminent technique for enrichment and unbiased detection of low abundant protein repertoires followed by mapping of their PPIs in cells and tissues [34–36].

Hence, considering the first outlook of the functional relevance of the Kv1.6 channel in the ophthalmic artery in our previous study [12] and

importantly, the virtually unexplored Kv1.6 channel interactome nor their potential roles in ocular vascular beds, the current study took advantage of the state-of-the-art MS technique to first, comprehensively map the whole proteome of the murine retrobulbar ophthalmic artery and, neuroretina of two most common animal models in eye research, the mouse and rat. Next, we employed the AP-MS platform to enrich the Kv1.6 channel and specifically identify the putative interacting protein partners in the ophthalmic artery. This was followed by the determination of Kv1.6 channel-interactome in the retina in an endeavour to also confirm the existence of this channel subtype in this tissue based on previous investigations [24,25] and identify its binding partners. Finally, the Kv1.6 channel-interacting proteins were subjected to rigorous *in silico* bioinformatics analyses to elucidate their molecular signatures and dissect cell signalling pathways with translational potential in both ocular vascular beds. This study provided the first in-depth insight into the global proteome landscape and elucidated the interactome of Kv1.6 channel in the ophthalmic artery and retina of rodents; thereby, extending our previous findings [12].

2. Materials and methods

2.1. Animals

Male mice of the C57BL/6J background (The Jackson Laboratory, Bar Harbour, ME, USA) aged 13 to 22 weeks old and male Sprague-Dawley rats aged 13 weeks old (Janvier Labs, Le Genest Saint Isle, France) were used in this study. Animals were housed and acclimatized under standard conditions (12 h light/ dark cycle, temperature 22 ± 2 °C, relative humidity 55 ± 10 %) and given *ad libitum* access to food and water. Experiments using mice and rats were conducted in strict adherence to the Association for Research in Vision and Ophthalmology (ARVO) Statement for the Use of Animals in Ophthalmic and Vision Research and, followed the recommendations in the Animal Research: Reporting of *In Vivo* Experiments (ARRIVE) guidelines. Animal care complied with the institutional guidelines and Directive 2010/63/EU and, animal use conformed to the 3R principle to replace, reduce and refine. All animal experimental procedures were reviewed and approved by the institutional animal care committee [Translational Animal Research Centre (TARC)] of the University Medical Centre of the Johannes-Gutenberg University Mainz.

2.2. Experimental design

This study is divided into three main parts. In the first part, the whole proteome of murine ophthalmic artery and, neuroretina from mouse and rat were mapped. This was followed by the determination of the differentially abundant protein profiles of these different samples and species. In the second part of this study, the interactome of the Kv1.6 channel in each sample was determined using the affinity purification-mass spectrometry (AP-MS) approach, followed by the elucidation of the functionalities of different protein clusters with the use of statistical and bioinformatics analysis tools (Fig. 1). In the third part, we performed functional experiments to validate the native functionality of the recombinant Kv1.6 channel used in our current study using the potassium-binding benzofuran isophthalate (PBFI), a K^+ sensitive fluorescent dye. This was followed by Western blot analysis for further validation of the transmembrane cellular localization of this channel in the cells.

2.3. Sample preparation

Murine ocular tissue sample preparation was carried out as described in our previous study [33]. Briefly, mice were euthanized by CO_2 inhalation and their eyes were immediately enucleated with attached optic nerve and extraocular tissues in ice-cold Krebs-Henseleit buffer. The ophthalmic artery and neuroretina were isolated under a dissection microscope with fine tip-precision tweezers and Vannas capsulotomy scissors to remove all surrounding tissues and fat layers. The retinal samples of rats were carefully isolated in the similar manner. All tissue samples were immediately snap-frozen in liquid nitrogen following isolation and stored in −80 °C until use.

2.4. Tissue protein extraction

The ophthalmic artery and retinal samples from mice and rats were subjected to protein extraction procedure established in-house, which is catered specifically for ocular blood vessels [33,37]. Ophthalmic arterial samples were isolated from a total of 15 mice ($N = 15$ mice) and pooled from 5 mice per biological replicate to yield sufficient amount of proteins for analysis, while the retinal tissues were pooled from 2 animals per biological replicate ($N = 6$ animals/ species). In total, three biological replicates from each sample were used for subsequent experiments. Briefly, samples were homogenized in the T-PER Tissue Protein Extraction Reagent (Thermo Scientific Inc., Waltham, MA, USA; cat. no. 78510) and stainless steel beads using a bullet blender homogenizer (BBY24M Bullet Blender Storm, Next Advance Inc., Averill Park, NY, USA). The supernatant of the tissue homogenates was subjected to sample cleaning using 3 kDa centrifugal cut-off filters (Amicon Ultra 0.5 mL, Merck Millipore, Darmstadt, Germany). Protein concentration estimation of the resulting supernatant was determined with the bicinchoninic acid (BCA) protein assay kit (Pierce, Rockford, IL, USA).

2.5. Construct and cloning

HEK-293 T cells were authenticated by Eurofin genomics and cultured in Dulbecco's modified Eagle medium (DMEM; Gibco, Thermo Fisher Scientific Inc.; cat. no. 41965039) containing 10 % heat-inactivated fetal bovine serum (FBS; Gibco, Thermo Fisher Scientific.; cat. no. 26140087). Mouse potassium voltage-gated channel member 6 (Kcna6/ Kv1.6) cDNA was purchased from OriGene Technologies (Herford, Germany; cat. no. MC206669) and amplified for cloning into p3×FLAG-CMV-14 expression vector (Sigma-Aldrich, Taufkirchen, Germany; cat. no. E7908). Plasmid without insert was used as control.

HEK-293 T cells were harvested with 0.05 % trypsin/0.02 % EDTA in PBS and seeded into 15 cm cell culture dish (Greiner Bio-One, Frickenhausen, Germany) at a concentration of 1×10^5 cells in DMEM (20 mL/ dish, 6 dishes for each plasmid). One day after seeding, transfection reagent consisting 10 μg plasmid and 1 mM polyethilenimine, (PEI) in 2 mL PBS was added to the dishes and incubated for 10 min at room temperature. Cells were maintained in the incubator and two days post-transfection, cells were harvested by scraping and lysed in 10 mL of cell lysis buffer (25 mM Tris-HCl pH 7.2, 150 mM NaCl, 5 mM $MgCl_2$, 1 % NP-40, 5 % glycerol with protease inhibitor cocktail).

2.6. Affinity purification of Kv 1.6 channel-interacting proteins

Cell lysate was centrifuged (18, 000 xg, 4 °C, 15 min) and the supernatant was incubated with 600 μL of anti-FLAG M2 affinity beads (Sigma-Aldrich, Taufkirchen, Germany; cat. no. A2220) for 1 h at 4 °C. Then, the beads were washed with binding buffer (TBS, 50 mM Tris-HCl pH 7.5, 150 mM NaCl) and used as Kcna6 affinity beads. The affinity beads were subjected to SDS-PAGE followed by Coomassie Blue Staining (InstantBlue, Abcam, Berlin, Germany). Next, 50 μL of Kcna6 affinity beads were mixed with the ophthalmic artery and retinal tissue lysates from different animals in 500 μL of TBS and rotated overnight at 4 °C. The beads were washed with TBS (1 mL × 5) and the proteins were eluted with 0.1 M glycine buffer (pH 3.5, 100 μL x5). Eluted proteins were neutralized and subjected to mass spectrometry analysis.

2.7. Microfluorimetric measurement of K^+ with PBFI

The functionality of the Kv1.6 channel was validated using a

microfluorimetric measurement of K^+ concentration using PBFI as a K^+-sensitive fluorescent dye. Briefly, 293 T cells were cultured in DMEM in 12-well plates. After reaching 70 % confluency, cells were transiently transfected with 1 μg of 3×-FLAG-CMV-14 empty vector (EV) or 3×-FLAG-CMV-14 Kcna6 (Kcna6) for 24 h. The transfection set-up was as follows: 1 μg plasmid was mixed with 100 μL OptiMEM (Gibco, Thermo Fisher Scientific, Inc., cat. no. 11058021). Separately, 5 μL PEI was mixed with 100 μL OptiMEM, vortexed, incubated for 5 min at room temperature and added to the diluted DNA. The PEI/DNA mix was incubated for additional 10 min at room temperature and added lastly dropwise to the cells. Cells were incubated at 37 °C. The next day, 5 μM PBFI (Invitrogen, Thermo Fisher Scientific, Inc., cat. no. P1267MP) or DMSO as control were added to the cells. After 30 min incubation at 37 °C, 50 mM KCl to a total of 55.3 mM or sterile water as control were added to the cells and further incubated for 5 min at 37 °C. PBFI fluorescence intensity was measured using a Tecan plate reader at 340 nm excitation and 535 nm emission.

2.8. Plasma membrane protein isolation

The 293 T cells were cultured in DMEM in T175 flasks until reaching 70 % confluency. Cells were transfected with EV or Kcna6 following the previously described protocol. The transfection set-up was up-scaled to 250 μL PEI in 5 mL OptiMEM and 50 μg plasmid in 5 mL OptiMEM. A sample of cells was taken for whole cell lysing 24-h post-transfection and plasma membrane proteins were isolated from the remaining cells using the Minute™ Plasma Membrane Protein Isolation and Cell Fractionation Kit (Invent Biotechnologies, MN, USA, cat. no. SM-005). The resulting pellet of the plasma membrane proteins was resuspended in 0.5 % Triton X-100 in PBS.

2.9. Western blotting

Whole cells were lysed for 30 min on ice in cold radioimmunoprecipitation assay (RIPA) lysis buffer [250 mM NaCl, 50 mM tris (pH 7.5) 10 % glycerine, and 1 % Triton X-100] supplemented with 1:100 protease inhibitor cocktail (Merck Millipore, Darmstadt, Germany; cat. no. 539131) and phosphatase inhibitors sodium orthovandate (Na_3VO_4) and sodium fluoride (NaF), each 1 mM. This was followed by 15 min centrifugation at 14,000 rpm at 4 °C. Protein concentration of the whole cell lysates, the plasma membrane proteins and the cytoplasmic proteins were estimated using Pierce™ 660 nm Protein Assay Reagent (Thermo Fisher Scientific, cat. no. 22660). Proteins (15 μg) were mixed with 4× Laemmli buffer (277.8 mM tris pH 6.8, 44.4 % glycerol, 4.4 % SDS, 0.02 % Bromophenol blue) supplemented with 50 mM dithiothreitol (DTT) for western blotting. Samples were boiled at 95 °C for 5 min and loaded on 10 % acrylamide gel for SDS-PAGE and transferred onto a nitrocellulose membrane (GE Healthcare, cat. no. 10600001) for 1 h at 100 V. Directly following the transfer, protein bands were stained with 0.1 % Ponceau S in 5 % acetic acid and imaged with the BioRad ChemiDoc. Membranes were blocked with 3 % bovine serum albumin in PBS-T (1× PBS pH 7.2 containing 0.05 % Tween 20) for 1 h rocking at room temperature, followed by 3 × 5 min washing with PBS-T, and overnight incubation at 4 °C with the primary antibody diluted in PBS-T. The following day, membranes were washed 3 × 5 min with PBS-T and incubated for 1 h at room temperature with the HRP-conjugated secondary antibody. After another 3 × 5 min washing round with PBS-T, protein bands were visualized by enhanced chemiluminescence (Immobilon Western, Merck Millipore, cat. no. WBKLS0500) at the ChemiDoc. The list of antibodies used are listed in Supplementary Table S1.

2.10. Nano-liquid chromatography-electrospray ionization-MS/MS (nLC-ESI-MS/MS) analysis

The nano-LC system employed consisted of an EASY-nLC 1200 system (Thermo Scientific, Rockford, USA) with an Acclaim PepMap RSLC, 75 μm × 50 cm, nanoViper analytical column (Thermo Scientific, Rockford, USA). Briefly, solvent A, which consisted of LC-MS grade water with 0.1 % (v/v) formic acid, and solvent B consisting of LC-MS grade acetonitrile with 20 % (v/v) water and 0.1 % (v/v) formic acid were utilized. The run of the resulting gradient per sample added up to a total time of 90 min. 0–60 min: 5 % - 30 % B, 60–70 min: 30–100 % B, 70–90 min: 100 % B. The LC system was directly coupled with ESI-LTQ-Orbitrap-XL-MS system. Continuum mass spectra data were acquired on an ESI-LTQ-Orbitrap-XL MS (Thermo Scientific, Bremen, Germany). The general mass spectrometric conditions were as follows: positive-ion electronspray ionization mode, spray voltage set to 2.15 kV, heated capillary temperature set at 220 °C. The system was used in the data-dependent mode of acquisition, enabling automatic switches between MS and MS/MS modes. In MS mode the lock mass option was enabled. Internal recalibration was acquired in real time *via* polydimethylcyclosiloxane (PCM) ions (m/z 445.120025). The LTQ-Orbitrap was operated in a data-dependent mode of acquisition to automatically switch between Orbitrap-MS and LTQ-MS/MS acquisition. Survey full scan MS spectra (from m/z 300 to 2000) were acquired in the Orbitrap with a resolution of 60,000 at m/z 400 and a target automatic gain control (AGC) setting of 1.0×10^6 ions. The seven most intense precursor ions were sequentially isolated for fragmentation in the LTQ with a collision-induced dissociation (CID) fragmentation, the normalized collision energy (NCE) was set to 35 % with activation time of 30 ms with repeat count of 2 and dynamic exclusion duration of 210 s. The resulting fragment ions were recorded in the LTQ.

2.11. Label-free quantification (LFQ) analysis

The acquired continuum MS spectra were analysed by MaxQuant computational suite (version 2.0.3.0) and its built-in Andromeda search engine for peptide and protein identification [38–40]. The tandem MS spectra were searched against SwissProt database, as follows: *Homo sapiens*, accession date: 25 February 2022, annotated proteins: 20,375; *Mus musculus*, accession date: 25 February 2022, annotated proteins: 17,090; *Rattus norvegicus*, accession date: 25 February 2022, annotated proteins: 8137. Standard settings with peptide mass tolerance of ±30 ppm, fragment mass tolerance of ±0.5 Da, with ≥6 amino acid residues and only "unique peptides" that belong to a protein were chosen [38,40]. For limiting a certain number of peak matches by chance, a target-decoy-based false discovery rate (FDR) for peptide and protein identification was set to 0.01. Carbamidomethylation of cysteine was set as a fixed modification, while protein N-terminal acetylation and oxidation of methionine were defined as variable modifications, enzyme: trypsin and maximum number of missed cleavages: 2. The summary of MaxQuant parameters employed in the current analyses is tabulated in Supplementary Table S2.

2.12. Statistical and bioinformatics analysis

The output of the generated "proteingroups.txt" data from the MaxQuant analysis was utilized for statistical analysis with Perseus software (version 1.6.15.0) following data cleaning from reverse hits and contaminants. In the Perseus software, the statistical analysis was done as follows: First, a $\log_2$ transformation of all protein LFQ intensities was done and results were filtered to include only peptides with 3 valid measured values in at least one of the study groups. Missing values were subsequently imputated from a normal distribution in standard settings (width: 0.2, down shift: 1.8), enabling statistical analysis [40]. Significantly differentially abundant proteins were identified by Student's two-sample *t*-test with permutation-based FDR < 0.05. Unsupervised hierarchical clustering analysis was performed according to Euclidean distance (linkage = average; preprocess with k-means) to generate heat map of the differentially abundant proteins. For statistical evaluation of the APMS data, volcano plot for all the groups' comparison was

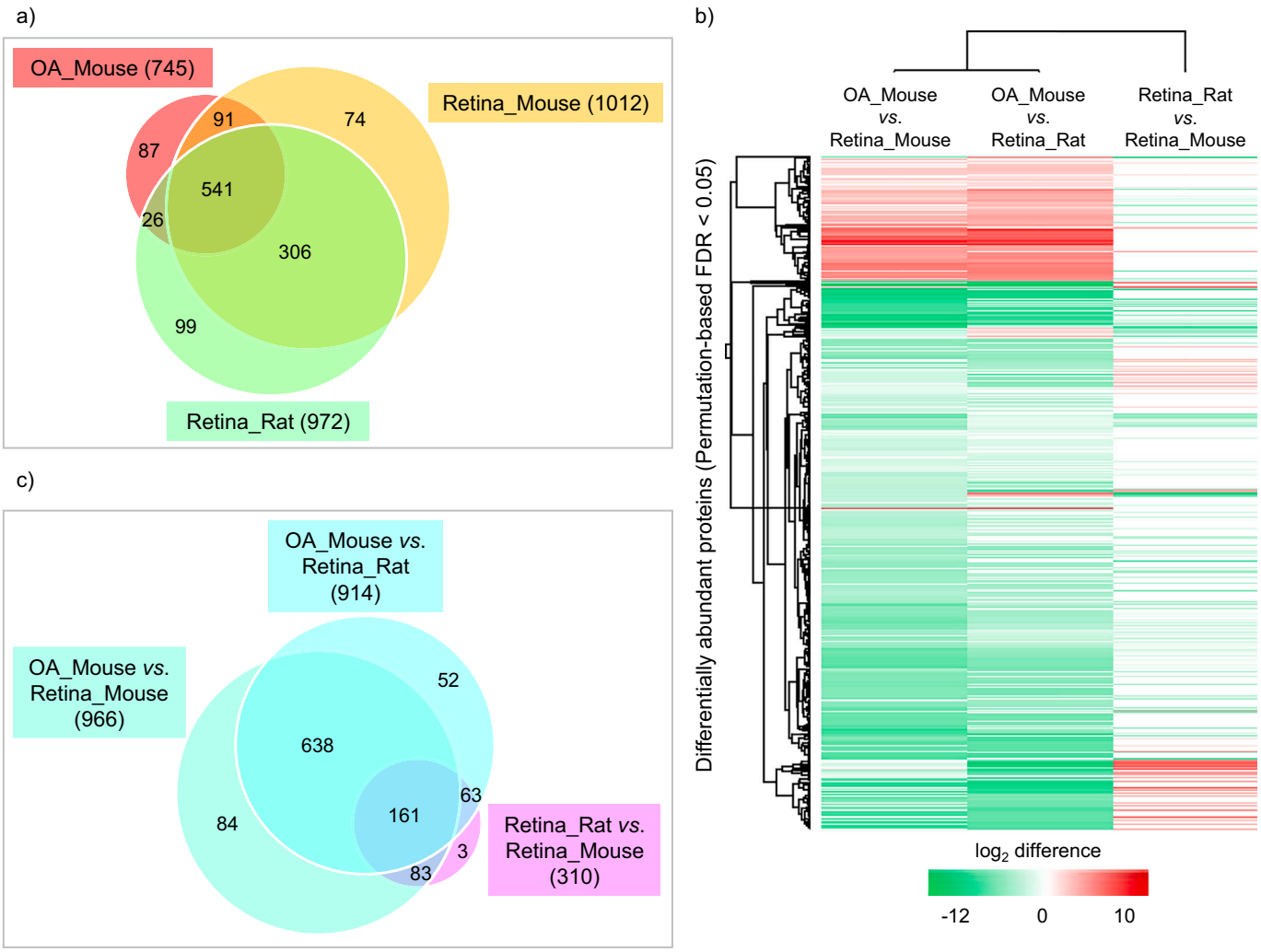

Fig. 2. Global proteome profiles of the ophthalmic artery and retina
(a) Venn diagram shows the total proteins identified in the murine ophthalmic artery and retina of different species. (b) Hierarchical clustering of the significantly (permutation-based FDR < 0.05) differentially expressed proteins of the murine and rat ophthalmic artery and retina represented in a heat map. The upregulated proteins are shown in red and the downregulated proteins are in green. (c) Venn diagram depicts the common and exclusive differentially expressed proteins in each comparison. Complete list of total proteins and differentially expressed protein are listed in Supplementary Tables S3 and S4, respectively. OA: ophthalmic artery.

generated bases on a Student's two-sided *t*-test with FDR < 0.05 and S0 > 0.1 to identify the significant Kv1.6 channel protein interactors. The gene names of the identified putative proteins in each group were used for subsequent functional annotation and pathways analyses employing the Ingenuity Pathway Analysis software (v01–04, IPA; Ingenuity QIAGEN Redwood City, CA) [41]. The IPA analysis unravelled the protein-protein interaction (PPI) networks and annotated the proteins according to their subcellular localization, identified the significantly affected canonical pathways, top biological functions, and predicted upstream regulators associated with the proteins identified to interact with the Kv1.6 channel in the ophthalmic artery and retina of different species. The top enriched canonical pathways, biological functions and upstream regulators implicated in each group were presented with *p*-value calculated using multiple testing correction and the significance threshold was also set at -log (*p*-value) > 1.3. In PPI networks, proteins molecules are represented by their corresponding gene names and, only PPIs that were experimentally observed and had direct interactions were used.

3. Results

3.1. Proteome profiles of the murine ophthalmic artery and neuroretina

In the first part of this study, the nLC-MS/MS proteomics analysis comprehensively mapped the proteome landscape of the murine ophthalmic artery and retina of two different rodents. Whole proteome map is important to identify and compare the Kv1.6 channel protein interactors that could be identified only *via* enrichment and affinity purification. A total of 745 proteins were identified from the murine ophthalmic artery, while the retina samples yielded a higher number of proteins from both animals (1012 and 972 proteins in the mouse and rat, respectively), at <1 % false discovery rate (FDR < 1 %) (complete protein list in Supplementary Table S3). A large majority of proteins (541 proteins) were found in all three samples, and as many as 306 proteins were commonly shared in the retinal samples regardless of the species of origin (Fig. 2a). It is noteworthy that approximately 7–12 % of the proteome of all three samples were only exclusive to the respective sample type, as demonstrated by the identification of 87, 74 and 99 proteins unique to the murine ophthalmic artery, retina of mouse and rat, respectively.

Next, the differential protein expression analysis demonstrated the

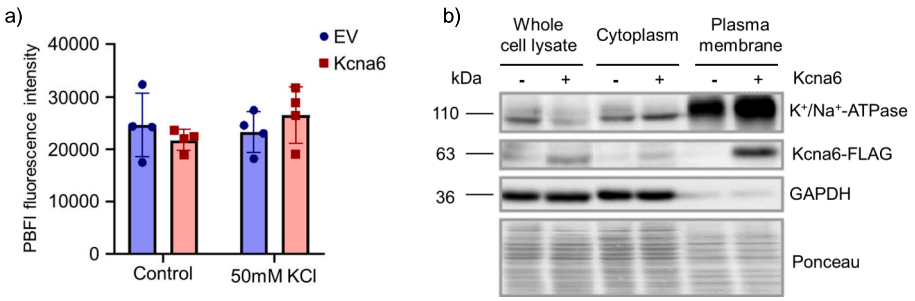

Fig. 3. Kv1.6 channel is expressed in the plasma membrane of 293 T cells and affects intracellular K^+ levels.
(a) The 293 T cells were transfected with 3×-FLAG-CMV-14 empty vector (EV; blue) or Kv1.6 channel (Kcna6; red) for 24 h and treated with 50 mM KCl or water (control) for 5 min. Intracellular K^+ levels were analysed by measuring PBFI fluorescence intensity. (b) Cell fractions of 293 T cells transfected with empty vector (−) or Kcna6 (+) were isolated and analysed by Western blotting. Kv1.6 protein was detected using anti-FLAG antibody, K^+/Na^+-ATPase was used as membrane protein control, GAPDH was used as whole cell and cytoplasmic protein control.

significant differences attributable to different ocular neuro-vascular tissues and also the animal species, with a total of 966 differentially expressed proteins in the murine ophthalmic artery compared to the retina (OA/RM), 914 proteins in the murine ophthalmic artery compared to the rat retina (OA/RR), and a lower number of 310 differentially expressed proteins in the retina of different rodents (RR/RM) (Supplementary Table S4). In all comparisons, a higher number of differentially expressed proteins were downregulated (798, 698 and 199

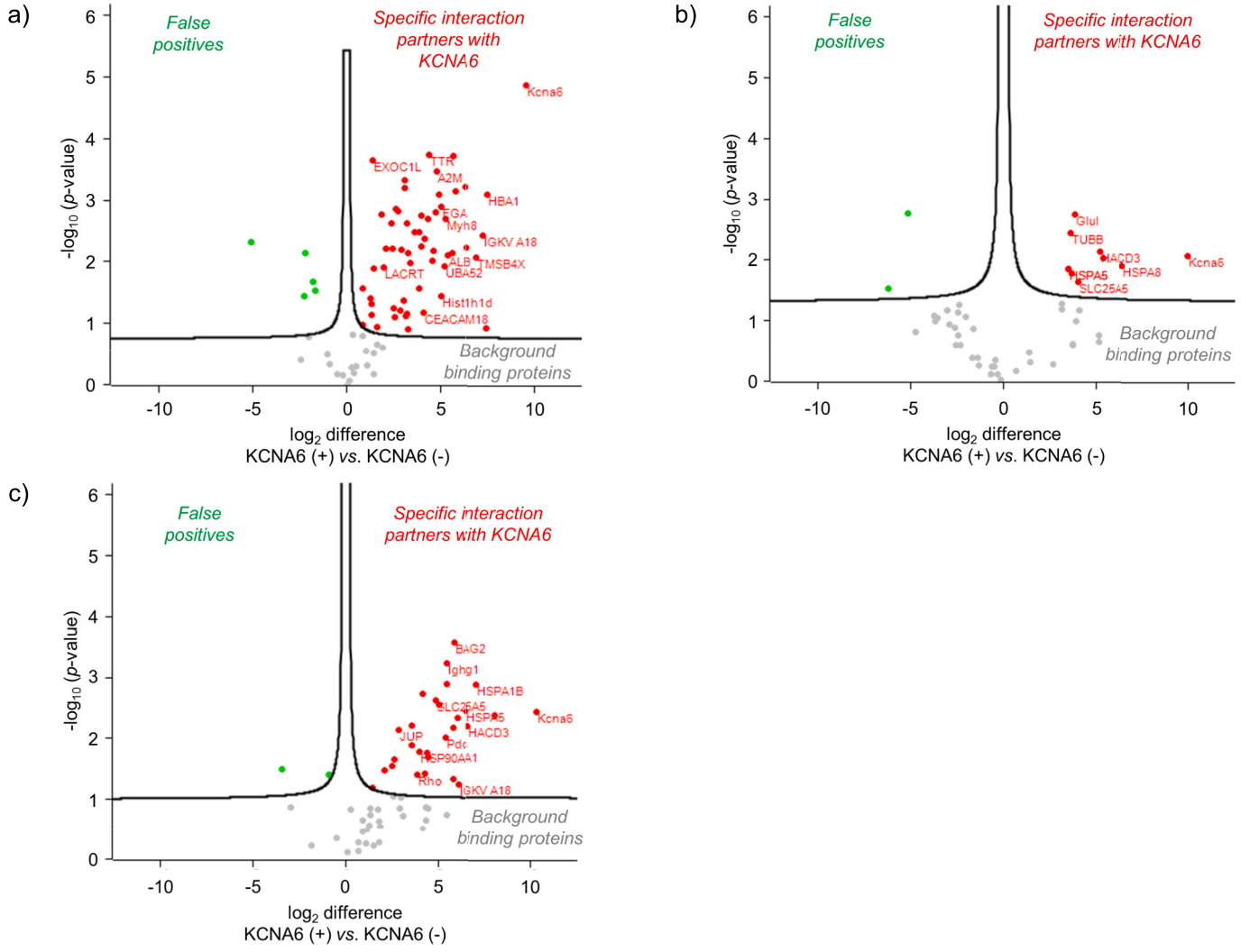

Fig. 4. The Kv1.6 channel interactome in the ophthalmic artery and retina
Volcano plots depict the Kv1.6-associated protein interactors in the (a) murine ophthalmic artery and retinal tissue of the (b) mouse and (c) rat. High-confident, significant interactors are represented by red dots and labelled with gene symbol, while the green dots are false positives. Non-specific binding proteins are shown as grey dots. The $\log_2$ difference in the bait *versus* control pull-downs is plotted on the x-axis and the $-\log_{10}$ (p value) is plotted on the y-axis. Significance threshold is at FDR 0.05 and S0 0.1. Complete set of proteins are listed in Supplementary Table S5 for the respective samples.

Fig. 5. Comparison analysis of the Kv1.6 channel interactome and the whole proteome of the ophthalmic artery and retina of different species
Venn diagrams show the number of Kv1.6-associated protein interactors identified from the total proteins and exclusive proteins identified only *via* AP-MS in the (a) murine ophthalmic artery and retinal tissue of the (b) mouse and (c) rat. Only a very small percentage ($\sim \leq 2$ %) of the Kv1.6 channel-interacting proteins detected with the AP-MS approach could be identified in the total proteome of all three samples. Complete lists of overlapping proteins and exclusive Kv1.6 channel-interactors are listed in Supplementary Table S6 for the respective samples. OA: ophthalmic artery.

proteins in OA/RM, OA/RR and RR/RM, respectively) compared to 168, 216 and 111 up-regulated proteins in the respective groups (Fig. 2b). However, as many as only 161 differentially expressed proteins were commonly identified in all comparisons, while the largest number of overlapping proteins (638 proteins) were found between OA/RM and OA/RR comparisons (Fig. 2c). Intriguingly, a higher number of exclusive proteins were identified in the murine ophthalmic artery and retina (OA/RM, 84 proteins) albeit the species similarity, compared to only 52 unique proteins in the murine ophthalmic artery and rat retina (OA/RR).

3.2. Cell transfection and affinity purification of Kv1.6 channel proteins

In the second part of this study, HEK-293 T cells expressing the target protein and FLAG-tagged affinity beads were used for affinity purification, followed by mass spectrometry and bioinformatics analyses to study the interactome of Kv1.6 channel in the ophthalmic artery and retina. To filter for false positives, plasmid without insert was used as control. After immunoprecipitation, the expression of the FLAG-tagged Kv1.6 was detected with SDS-PAGE of the cell lysate conjugated to anti-FLAG M2 affinity beads. The results confirmed the presence and absence of the Kv1.6 channel expression in the HEK-293 T cells with and without the insert, respectively, with the expected molecular weights (supplementary Fig. S1).

3.3. Validation of the recombinant Kv1.6 channel protein functionality and expression

Next, we used a set of orthogonal experimental approaches to characterize and validate the native functionality and cellular expression of the transmembrane Kv1.6 channel. First, the K^+-sensitive and selective fluorescent dye PBFI was employed to confirm the influx of K^+ *via* the recombinant Kv1.6 channel. The exposure of the cells expressing the recombinant Kv1.6 channel to 50 mM KCl resulted in increased intracellular fluorescence intensity compared to the empty vector, which corresponded to the K^+ ion binding to PBFI (Fig. 3a). Next, Western blot analysis was carried out to confirm the cellular localization of this channel subtype, which corresponded to its specific expression in the plasma membrane (Fig. 3b). As anticipated, no expression of the channel was observed in the empty vector without Kv1.6 channel, which was used as a negative control. The expression profiles of both positive control proteins, K^+/Na^+-ATPase and GAPDH, showed their respective expressions in the plasma membrane and, whole cell lysate and cytoplasm, respectively. Collectively, these findings proved that the recombinant Kv1.6 channel used in this study is a functional transmembrane

Table 1
Identified Kv1.6-associated proteins in the murine ophthalmic artery.

Protein ID	Protein name	Gene symbol	*p*-Value	Log_2 difference
Q61923	Potassium voltage-gated channel subfamily A member 6	Kcna6	1.36E-05	9.49
P69905	Hemoglobin subunit alpha	HBA1	7.84E-04	7.46
O35166	Golgi SNAP receptor complex member 2	Gosr2	1.15E-01	7.37
A2NJV5	Ig kappa chain V-II region RPMI 6410	IGKV A18	3.73E-03	7.23
P62328	Thymosin beta-4	TMSB4X	8.31E-03	6.87
P01868	Ig gamma-1 chain C region secreted form	Ighg1	6.00E-04	6.28
P01834	Ig kappa chain C region	IGKC	7.06E-04	5.73
Q9ULQ0	Striatin-interacting protein 2	STRIP2	1.86E-04	5.62
P68871	Hemoglobin subunit beta	HBB	7.02E-03	5.59
P02768	Serum albumin	ALB	7.55E-03	5.35
P04462	Myosin-8	Myh8	1.96E-03	5.24
P62987	Ubiquitin-60S ribosomal protein L40	UBA52	1.16E-02	5.15
P02671	Fibrinogen alpha chain	FGA	1.24E-03	4.97
P43277	Histone H1.3	Hist1h1d	3.59E-02	4.96
P02765	Alpha-2-HS-glycoprotein	AHSG	7.83E-04	4.84
P01023	Alpha-2-macroglobulin	A2M	3.28E-04	4.76
P01009	Alpha-1-antitrypsin	SERPINA1	1.54E-03	4.67
P63261	Actin, cytoplasmic 2	ACTG1	6.58E-03	4.56
P42167	Lamina-associated polypeptide 2, isoforms beta/gamma	TMPO	9.30E-03	4.50
P02766	Transthyretin	TTR	1.80E-04	4.32
Q02413	Desmoglein-1	DSG1	1.95E-03	4.27
P0DP25	Calmodulin-3	CALM3	4.07E-03	4.09
A8MTB9	Carcinoembryonic antigen-related cell adhesion molecule 18	CEACAM18	6.57E-02	4.05
P02647	Apolipoprotein A-I	APOA1	1.75E-03	3.94
P01876	Ig alpha-1 chain C region	IGHA1	5.57E-03	3.92
P01024	Complement C3	C3	3.29E-03	3.84
O54724	Polymerase I and transcript release factor	Ptrf	2.63E-02	3.82
P11142	Heat shock cognate 71 kDa protein	HSPA8	3.20E-03	3.60
P00762	Anionic trypsin-1	Prss1	1.03E-02	3.35
P15999	ATP synthase subunit alpha, mitochondrial	Atp5a1	6.96E-03	3.21
P10412	Histone H1.4	HIST1H1E	6.94E-02	3.19
Q91XV3	Brain acid soluble protein 1	Basp1	2.32E-03	3.16
P15864	Histone H1.2	Hist1h1c	7.37E-02	3.10
P17066	Heat shock 70 kDa protein 6	HSPA6	4.67E-04	3.07
P43276	Histone H1.5	Hist1h1b	6.22E-04	3.07
P80188	Neutrophil gelatinase-associated lipocalin	LCN2	4.19E-02	2.99
P02675	Fibrinogen beta chain	FGB	6.29E-03	2.85
Q09666	Neuroblast differentiation-associated protein AHNAK	AHNAK	1.50E-03	2.68
P10599	Thioredoxin	TXN	1.38E-03	2.61
P06733	Alpha-enolase	ENO1	7.80E-02	2.50
P0DOY3	Ig lambda-6 chain C region	IGLC6	5.62E-02	2.47
P01040	Cystatin-A	CSTA	5.99E-03	2.38
Q63918	Serum deprivation-response protein	Sdpr	2.31E-03	2.37
Q16531	DNA damage-binding protein 1	DDB1	5.97E-03	2.05
Q9GZZ8	Extracellular glycoprotein lacritin	LACRT	1.19E-02	1.92
O75449	Katanin p60 ATPase-containing subunit A1	KATNA1	1.68E-03	1.82
Q15058	Kinesin-like protein KIF14	KIF14	1.13E-01	1.56
P04264	Keratin, type II cytoskeletal 1	KRT1	1.26E-02	1.40
A0A1B0GW35	Exocyst complex component 1-like	EXOC1L	2.17E-04	1.37
P31025	Lipocalin-1	LCN1	7.22E-02	1.28
P48668	Keratin, type II cytoskeletal 6C	KRT6C	4.82E-02	1.28
P13645	Keratin, type I cytoskeletal 10	KRT10	3.89E-02	1.22
P35908	Keratin, type II cytoskeletal 2 epidermal	KRT2	2.62E-02	0.84
P35527	Keratin, type I cytoskeletal 9	KRT9	1.04E-01	0.84

protein that effectively mediates the flow of K^+ across cell membrane.

3.4. Identification of Kv1.6-interacting proteins in the murine ophthalmic artery and neuroretina

Following affinity purification, the identity of the interacting protein partners of Kv1.6 channel in the murine ophthalmic artery and neuroretinal tissues of the two different rodent species were defined using the label-free nLC-MS/MS-based proteomics approach. The total proteins identified in all samples are in listed in Supplementary Table S5. Of the identified putative protein interactors of the Kv1.6 channel, a total of 54 proteins were found to be significantly enriched (FDR < 0.05) in the murine ophthalmic artery (Fig. 4a, Table 1), 9 proteins in the murine retina (Fig. 4b, Table 2) and 28 proteins in the rat retina (Fig. 4c, Table 3). Remarkably, only a very small percentage of these Kv1.6 channel-interacting proteins were identified in the total proteome of all three samples, with ~2 % (15 proteins) of the whole ophthalmic arterial proteome (Fig. 5a, Supplementary Table S5a), as low as ~0.4 % (4 proteins) of the murine retinal (Fig. 5b, supplementary Table S5b) and ~1 % (10 proteins) of the rat retinal proteome (Fig. 5c, Supplementary Table S5c). There was a large percentage of proteins that were only identified following enrichment and affinity purification, as evidenced by the identification of ~72 % (39 proteins), ~56 % (5 proteins) and ~64 % (18 proteins) in the murine ophthalmic artery and retina of mouse and rat, respectively (Fig. 5). Complete lists of overlapping proteins and exclusive Kv1.6 channel-interactors are listed in supplementary Table S6 for the respective samples.

Table 2
Identified Kv1.6-associated proteins in the murine retina.

Protein ID	Protein name	Gene symbol	*p*-value	Log_2 difference
Q61923	Potassium voltage-gated channel subfamily A member 6	Kcna6	8.34E-03	9.91
P11142	Heat shock cognate 71 kDa protein	HSPA8	1.23E-02	6.42
P0DMV9	Heat shock 70 kDa protein 1B	HSPA1B	9.09E-03	5.37
Q9P035	Very-long-chain (3*R*)-3-hydroxyacyl-CoA dehydratase 3	HACD3	7.11E-03	5.16
P05141	ADP/ATP translocase 2	SLC25A5	2.20E-02	3.98
P09606	Glutamine synthetase	Glul	1.72E-03	3.79
P01868	Ig gamma-1 chain C region secreted form	Ighg1	1.62E-02	3.64
P07437	Tubulin beta chain	TUBB	3.51E-03	3.58
P11021	78 kDa glucose-regulated protein	HSPA5	1.35E-02	3.43

Among these Kv1.6-interacting proteins, only three proteins comprising heat shock cognate 71 kDa protein (HSPA8), Ig gamma-1 chain C region secreted form (Ighg1) and potassium voltage-gated channel subfamily A member 6 (Kcna6/ Kv1.6) were found in all samples, while as many as 45 and 13 proteins were found to be exclusive to the ophthalmic artery and rat retina, respectively (Fig. 6a). Only six common proteins were found in retinal samples of both species, and also in both ophthalmic artery and rat retina. Intriguingly, there were no common Kv1.6-interacting proteins identified in the murine samples of both ophthalmic artery and retina albeit the species similarity apart from the three proteins (HSPA8, Ighg1 and Kcna6), which were also identified in the rat retina. The log_2 difference profiles of these three common protein interactors in all samples showed that the expression of the Kv1.6 channel was higher than the other two proteins in all samples, which confirms the successful enrichment of this channel subtype for identification using the MS approach (Fig. 6b). The exemplary profiles of five of the most significant Kv1.6 channel-interacting proteins exclusive to the ophthalmic artery comprised alpha-2-macroglobulin (A2M), actin cytoplasmic 2 (ACTG1), myosin-8 (MYH8), thymosin beta-4 (TMSB4X) and transthyretin (TTR) (Fig. 6c). Interestingly, the exemplary profiles of four of the Kv1.6-interacting partners identified to be exclusively significant to the retinal tissue samples regardless of the species, which comprised the heat shock 70 kDa protein 1B (HSPA1B), 78 kDa glucose-regulated protein (HSPA5), ADP/ATP translocase 2 (SLC25A5) and tubulin beta chain (TUBB), were all highly expressed in the rat retina compared to the murine counterpart (Fig. 6d). The large majority of the protein interactors were localized in the cytoplasm (ophthalmic artery: 37.0 %, murine retina: 77.8 % and rat retina: 64.3 %) and most of these proteins comprised enzymes (ophthalmic artery: 14.8 %, murine retina: 55.6 % and rat retina: 35.7 %) (supplementary Fig. S2).

3.5. Functional annotation of the protein partners of Kv1.6 channel

Next, we sought to determine the comparative physiological functionalities and biological processes attributed to the Kv1.6-associated interaction protein partners in each group. First, canonical pathway analysis demonstrated that the proteins associated with the Kv1.6 channel in all samples were significantly implicated in the glucocorticoid receptor signalling, BAG2 signalling pathway, unfolded protein response and protein ubiquitination pathway (Fig. 7a). The Kv1.6 channel protein partners found in the murine ophthalmic artery were significantly implicated in the regulation of the acute phase response signalling ($p = 2.27 \times 10^{-10}$), liver X receptor-retinoid X receptor (LXR/RXR) activation ($p = 8.93 \times 10^{-9}$), coagulation system ($p = 9.97 \times 10^{-7}$) and integrin-linked kinase (ILK) signalling ($p = 9.61 \times 10^{-3}$). Most of the proteins involved in the ubiquitination pathway (Fig. 7b) and glucocorticoid receptor signalling (Fig. 7c) comprised a cluster of heat shock proteins (HSPA1B, HSPA5, HSPA6, HSPA8, and HSP90AA1) in addition to a cluster of keratins in the latter (KRT1, KRT2, KRT6C, KRT9 and KRT10). On the contrary, the Kv1.6 channel-interacting proteins involved in acute phase response signalling in the ophthalmic artery were composed mainly of transporter proteins [apolipoprotein A-

Table 3
Identified Kv1.6-associated proteins in the rat retina.

Protein ID	Protein name	Gene symbol	*p*-value	Log_2 difference
Q61923	Potassium voltage-gated channel subfamily A member 6	Kcna6	3.58E-03	10.27
P17066	Heat shock 70 kDa protein 6	HSPA6	4.19E-03	8.06
P0DMV9	Heat shock 70 kDa protein 1B	HSPA1B	1.29E-03	7.04
Q9P035	Very-long-chain (3*R*)-3-hydroxyacyl-CoA dehydratase 3	HACD3	6.13E-03	6.56
P11021	78 kDa glucose-regulated protein	HSPA5	3.46E-03	6.43
A2NJV5	Ig kappa chain V-II region RPMI 6410	IGKV A18	5.61E-02	6.02
P48668	Keratin, type II cytoskeletal 6C	KRT6C	4.49E-03	5.98
O95816	BAG family molecular chaperone regulator 2	BAG2	2.62E-04	5.81
P11142	Heat shock cognate 71 kDa protein	HSPA8	6.54E-03	5.77
P62987	Ubiquitin-60S ribosomal protein L40	UBA52	4.59E-02	5.73
P01868	Ig gamma-1 chain C region secreted form	Ighg1	5.75E-04	5.40
P05023	Sodium/potassium-transporting ATPase subunit alpha-1	ATP1A1	1.23E-03	5.39
P20942	Phosducin	Pdc	9.61E-03	5.33
P07437	Tubulin beta chain	TUBB	2.69E-03	4.99
P05141	ADP/ATP translocase 2	SLC25A5	2.36E-03	4.81
P02091	Hemoglobin subunit beta-1	Hbb	1.98E-02	4.37
P31689	DnaJ homolog subfamily A member 1	DNAJA1	1.70E-02	4.34
Q07065	Cytoskeleton-associated protein 4	CKAP4	3.73E-02	4.23
P09606	Glutamine synthetase	Glul	1.79E-03	4.10
P07900	Heat shock protein HSP 90-alpha	HSP90AA1	1.62E-02	3.93
P51489	Rhodopsin	Rho	3.84E-02	3.82
P01837	Ig kappa chain C region	Igkc	1.27E-02	3.51
P04843	Dolichyl-diphosphooligosaccharide–protein glycosyltransferase subunit 1	RPN1	5.94E-03	3.49
P14923	Junction plakoglobin	JUP	7.14E-03	2.79
P06576	ATP synthase subunit beta, mitochondrial	ATP5B	2.11E-02	2.57
P46462	Transitional endoplasmic reticulum ATPase	Vcp	2.79E-02	2.48
Q91XV3	Brain acid soluble protein 1	Basp1	3.21E-02	2.05
P35908	Keratin, type II cytoskeletal 2 epidermal	KRT2	6.24E-02	1.39

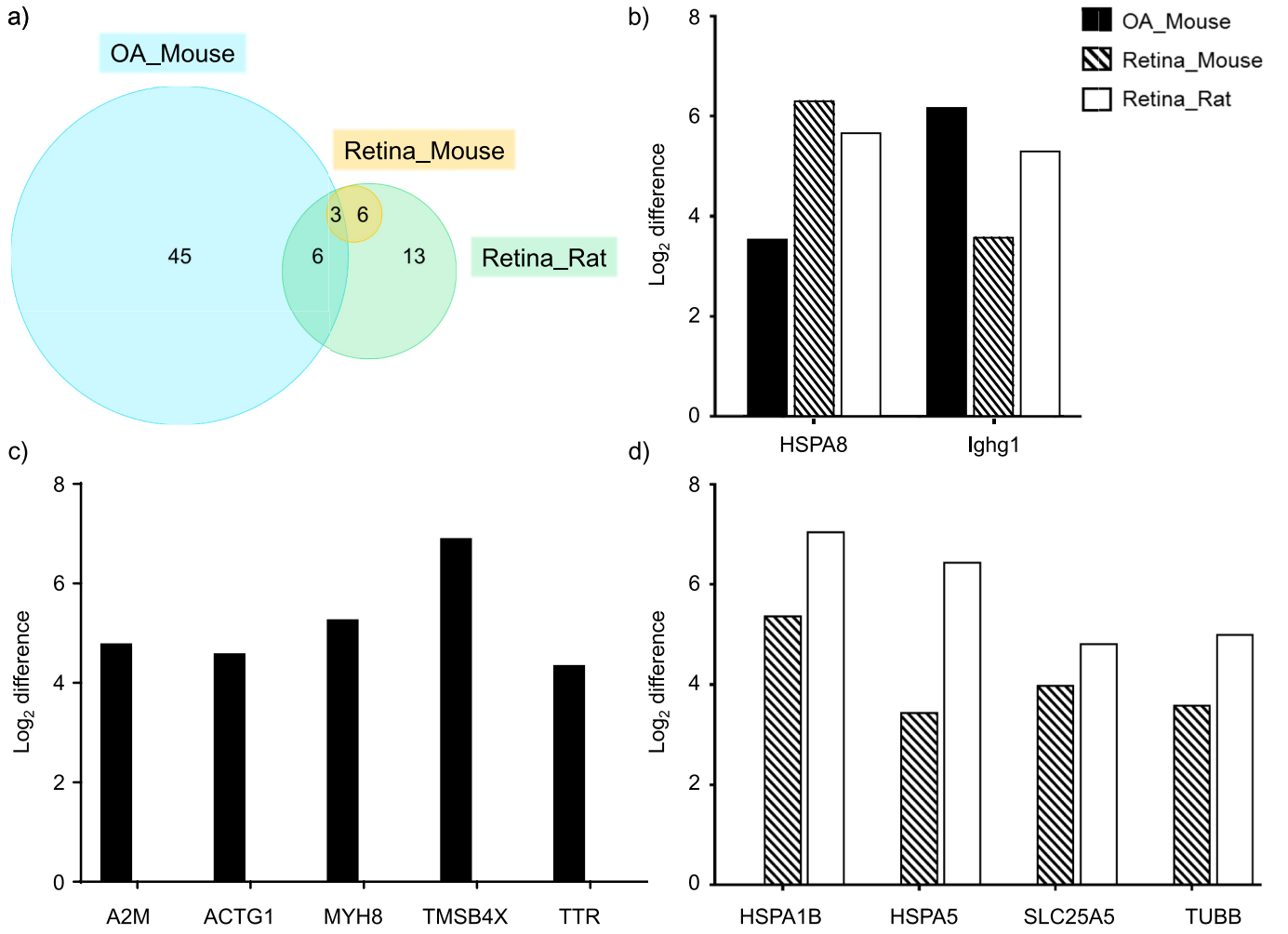

Fig. 6. Comparison of the protein partners of Kv1.6 channel between the ophthalmic artery and retina of different species
(a) Venn diagram highlights the total number of protein Kv1.6 channel interactors identified in each group. Only three proteins were found to be the common protein partners in all the samples and species investigated, while as many as 45 and 13 proteins were shown to be exclusive to the murine ophthalmic artery and rat retina, respectively. There were no exclusive proteins identified in the murine retinal samples. Bar charts represent the $\log_2$ difference of (b) three common interactors in all samples composed of HSPA8, Ighg1 and Kcna6/ Kv1.6, (c) five selected proteins found to be exclusive only in the ophthalmic artery and, (d) four proteins identified to interact with the Kv1.6 channel only in the retina samples regardless of the species.

I (APOA1), A2M, serum albumin (ALB) and TTR] (Fig. 7d), while all three proteins in the ILK signalling comprising TMSB4X, MYH8 and ACTG1 were exclusively identified only in the ophthalmic artery (Fig. 7e).

This analysis was followed by specific investigation into the biological functions attributable to the protein networks of the Kv1.6 channel to better understand the molecular mechanisms underlying the interactomes between the groups. The top functions associated with the Kv1.6-interacting proteins comprised apoptosis, apoptosis of photoreceptors, cell viability, chaperone mediated autophagy, development of vasculature, endoplasmic reticulum stress response, flux of Ca^{2+}, inflammatory response, necrosis and transport of molecule (Fig. 8a). Among these, the most significantly implicated functions in all samples reflect the cluster of proteins involved in necrosis and transport of molecule. A striking feature of these results demonstrated that several diseases and biological functions were only attributable to retinal proteins in both species such as apoptosis of photoreceptors (murine retina: $p = 1.11 \times 10^{-2}$; rat retina: $p = 5.11 \times 10^{-4}$), cell viability (murine retina: $p = 1.24 \times 10^{-2}$; rat retina: $p = 4.19 \times 10^{-4}$), chaperone mediated autophagy (murine retina: $p = 3.07 \times 10^{-3}$; rat retina: $p = 3.58 \times 10^{-5}$) and endoplasmic reticulum stress response (murine retina: $p = 3.23 \times 10^{-3}$; rat retina: $p = 1.95 \times 10^{-7}$). On the other hand, development of vasculature ($p = 6.13 \times 10^{-3}$), flux of Ca^{2+} ($p = 2.40 \times 10^{-3}$) and inflammatory response ($p = 2.09 \times 10^{-3}$) were found to be only associated with the ophthalmic arterial protein interactors. It was noteworthy that necrosis (z-score = −1.511 in ophthalmic artery, −1.577 in murine retina and − 1.604 in rat retina) and apoptosis (z-score = −1.531 in ophthalmic artery and − 2.205 in rat retina) were inhibited, while the transport of molecule (z-score = 3.097 in ophthalmic artery and 2.216 in rat retina) and cell viability (z-score = 1.927 in murine retina and 2.187 in rat retina) functions were activated by different clusters of Kv1.6 channel-interacting protein partners in the ophthalmic arterial and retinal samples (Fig. 8b).

The exemplary gene heatmap of apoptosis (Fig. 8c) and molecular transport (Fig. 8d) demonstrated the involvement of a large majority of the protein partners identified in all samples. On the other hand, a cluster of identified interactors of Kv1.6 channel were shown to be associated with specific functions only in the ophthalmic artery, namely development of vasculature and (Fig. 8e) and flux of Ca^{2+} (Fig. 8f). The latter is exemplified as a gene heatmap, which showed that different transporters were among the proteins involved in this physiological functionality of the ophthalmic artery. Endoplasmic reticulum (ER) stress response in the retinal samples highlighted the involvement of HSPA1B, HSPA5, HSPA6, HSP90AA1, DnaJ homolog subfamily A

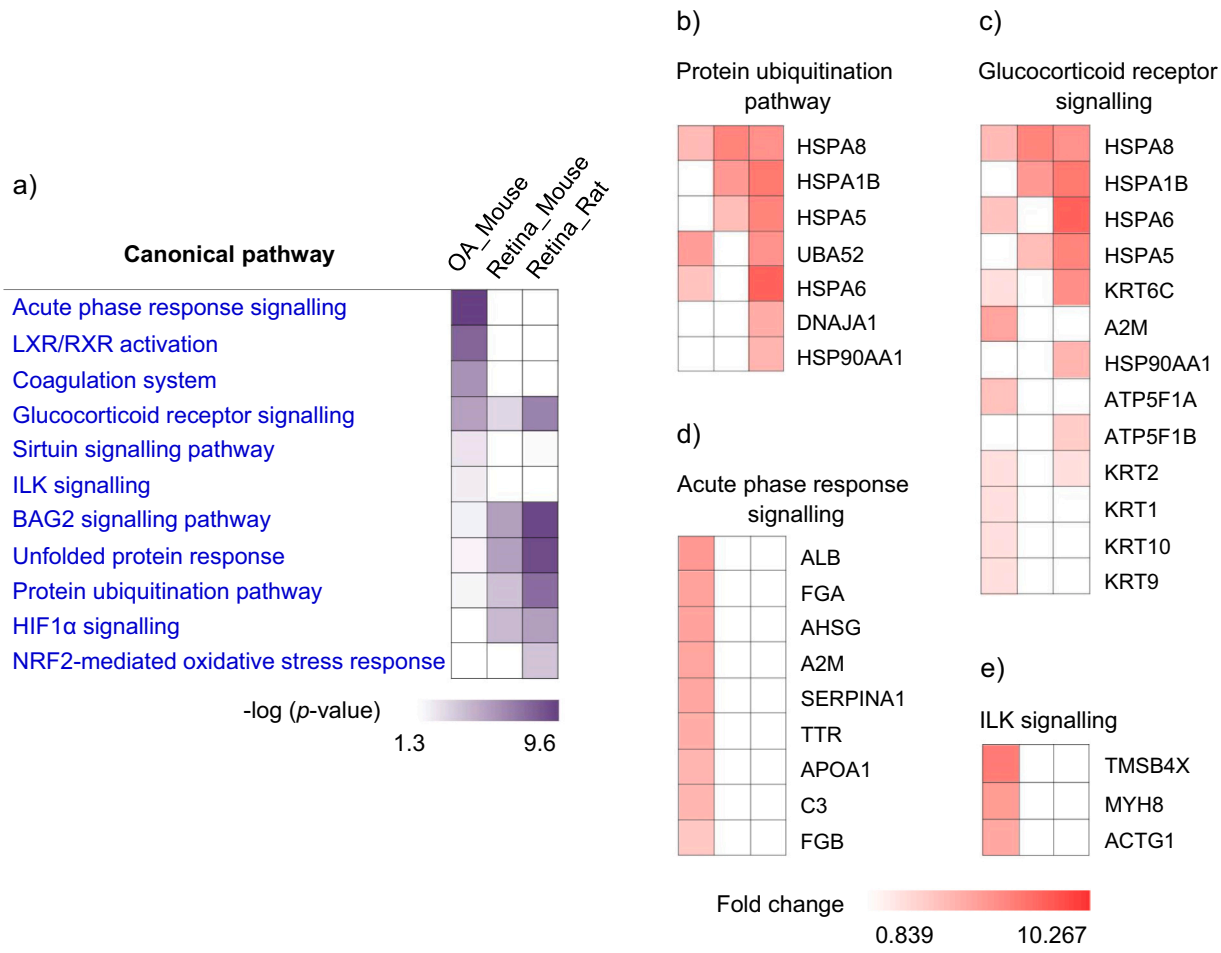

Fig. 7. Functional annotation of the top significant canonical pathways of Kv1.6 channel interactome
(a) The comparison of the top significantly [−log (*p*-value) > 1.3] enriched canonical pathways of the proteins identified as Kv1.6 channel interactors between the ophthalmic artery and retinal tissues of different species. Exemplary protein expression profiles in each group associated with respective pathways represented by (b) protein ubiquitination (c) glucocorticoid receptor signalling (d) acute phase response signalling and (e) ILK signalling. The intensity of the colour red indicates the degree of $\log_2$ fold change of each protein.

member 1 (DNAJA1) and transitional endoplasmic reticulum ATPase (VCP) (Fig. 8g).

3.6. *Upstream regulators of the Kv1.6 channel-associated proteins*

In our endeavour to further dissect the therapeutic potential and define the hierarchy of a molecular interactome of the Kv1.6 channel-protein partners in these ocular neuro-vascular beds, we performed an additional *in silico* upstream regulator analysis in the IPA computational suite. This analysis revealed four top most significant upstream regulators in all samples, which comprised microtubule associated protein tau (MAPT), presenilin-1 (PSEN1), amyloid beta precursor protein (APP) and interferon gamma (IFNG) (Fig. 9a); each predicted to act upon different sets of target molecules, likely to mediate various biological effects. Intriguingly, several transcription regulators such as forkhead box A2 (FOXA2; p-value $= 1.22 \times 10^{-6}$), signal transducer and activator of transcription 3 (STAT3; p-value $= 2.49 \times 10^{-4}$), the receptor for the cytokine oncostatin M (OSMR; p-value $= 3.87 \times 10^{-4}$) and tumour protein p73 (tp73) (p-value $= 2.67 \times 10^{-2}$) were demonstrated to regulate only the protein interactors in the ophthalmic artery (Fig. 9a). Similarly in the retina, the regulator effects analysis predicted that the major prion protein (PRNP) is involved in the regulatory network of only retinal proteins in both species (Fig. 9b). However, a big cluster of proteins in all three samples were shown to be regulated by common regulators such as APP (Fig. 9c) and tumour protein p53 (tp53) (Fig. 9d). The exemplary regulation profile of the activated protein-coding transcription regulator, FOXA2, demonstrated that ~50 % of the regulated ophthalmic arterial proteins composed of transporters such as A2M, ALB, APOA1 and TTR, while the other interactors were a peptidase (C3) and a serine proteinase inhibitor, SERPINA1 (Fig. 9e).

4. Discussion

This study is, to the best of our knowledge, the foremost in-depth investigation that mapped the complex whole proteome landscape and subsequently, elucidated the Kv1.6 channel interactome in two different ocular neuro-vascular tissues, and importantly, in different rodent species. The first finding of this study was the identification of three common Kv1.6 channel interactors in all samples following enrichment, which composed of heat shock cognate 71 kDa protein (HSPA8), Ighg1 and importantly, the elusive Kv1.6 channel (Kcna6) itself using the AP-MS approach. The HSPA8 protein, also commonly known as the heat shock cognate 70 (Hsc70) protein, is a constitutively expressed cytosolic protein with molecular chaperone functions that dictate protein triage decisions and influence cellular homeostasis [42,43]. A unique characteristic of this protein is its ability to interact with various ion channels such as the transient receptor potential vanilloid type 1 (TRPV1) channel and acid-sensing ion channel (ASIC), which play an important role in vascular remodelling [43,44]. Notwithstanding its universal expression and functionality, this main housekeeping heat shock protein is also

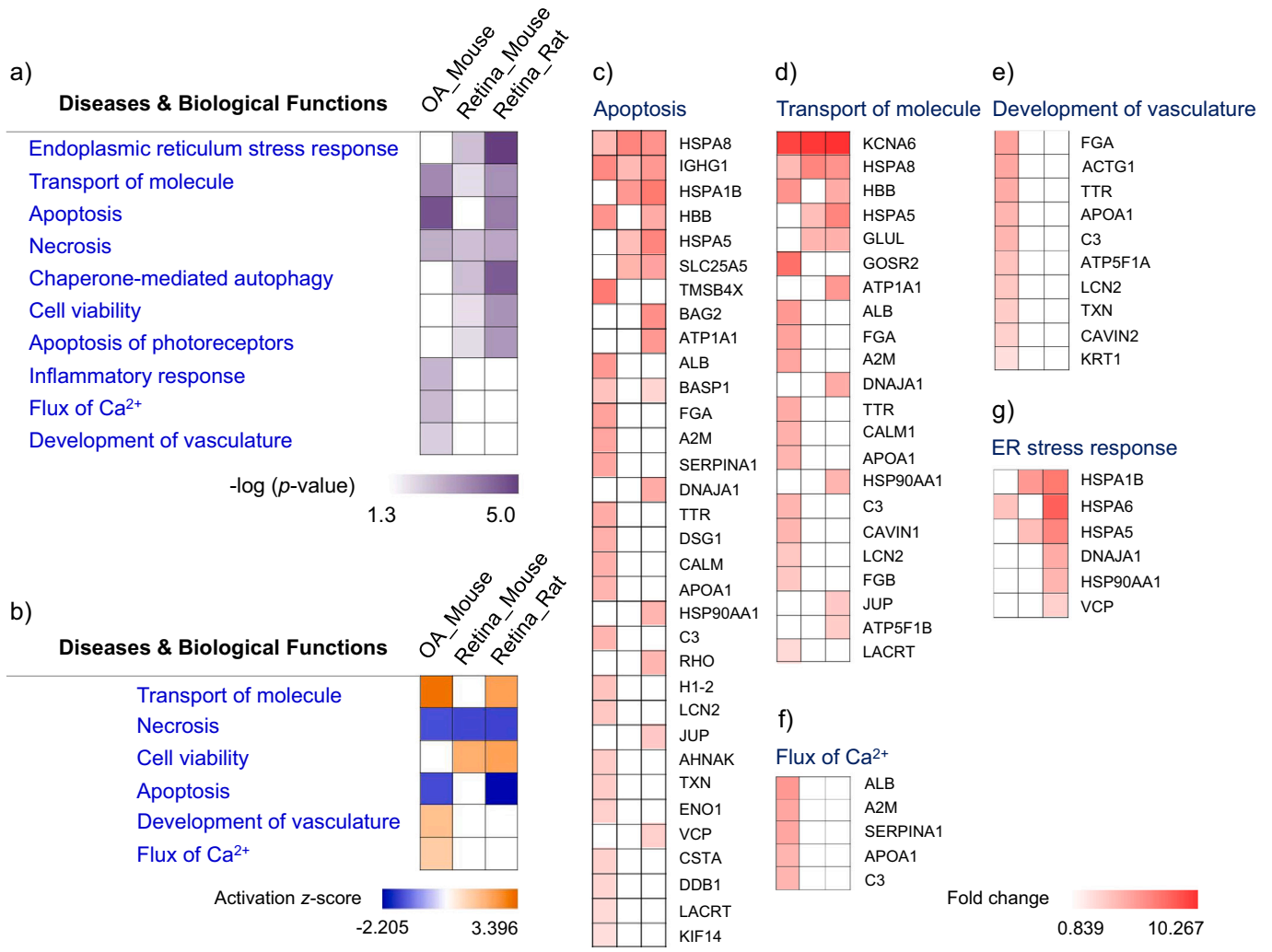

Fig. 8. Classification of the interacting partners of Kv1.6 channel according to top disease and biological functions
(a) Heat map depicts the top biological functions attributable to the protein interactors of the Kv1.6 channel in both ophthalmic artery and retina classified according to the significance threshold [−log (*p*-value) > 1.3] and the (b) activation *z*-score shown as blue (inhibition) and orange (activation), which were determined by IPA. The exemplary protein profiles of the biological functions implicated in all samples is represented by (c) apoptosis and (d) transport of molecule, while (e) development of vasculature and (f) flux of Ca^{2+} were only shown to be solely attributed to the ophthalmic artery and (g) ER stress response was attributed to a majority of retinal proteins.

notable for its involvement in the ubiquitin-proteasome pathway to preserve cellular proteostasis [42,45]. This comes as no surprise because polyubiquitin is recognized as a heat shock responsive gene in an HSF1-dependent manner [46,47]. The regulation of APP is dependent on the transcriptional regulation of HSF [48], which corroborated with our current finding that both HSF1 and APP are among the significant upstream regulators associated with several of the key interactors of Kv1.6 channel in both ophthalmic artery and the retina of all species.

Mutations in the *APP* and *PSEN1* genes are well-recognized to lead to early onset of a prototypical neurodegenerative disease, Alzheimer's [49–51]. Of note, the voltage-gated potassium channels, particularly the Kv1.3 channel, are shown to have a direct role in the microglial cell proliferation and also to modulate the latter's activity during neuroinflammation [52,53]. Since the retina is a neurovascular unit with similar attributes to the central nervous system, the significant association of both upstream regulators (APP and PSEN1) to the Kv1.6 channel-protein partners in the present investigation can be conceptually extrapolated to the same regulatory pattern in the eye. Both regulators were also found to regulate a cluster of Kv1.6-interacting proteins in the ophthalmic artery. On one hand, PSEN1 has an important role in the maintenance of blood vessel integrity by regulating integrin-mediated adhesion to extracellular matrix [54,55], which can be reflected in the significant regulation of the ILK signalling in the ophthalmic artery in our study. On the other hand, PSEN1 has a tangible influence on downstream protective effects during stress and apoptosis [56–59]; both of which were highlighted in our findings that showed the canonical involvement of ER stress response in the retina and apoptosis in both vascular beds. One of the members of the heat shock protein family that was found only in the retinal PPI network in this study was the HSPA5. An interesting feature of this protein is that its localization is restricted to the endoplasmic reticulum (ER) [60]. An investigation by Zhu and colleagues demonstrated that the Kv1.6 channel was distinctly enriched in the ER of rat astrocytes [9]. Moreover, the expression of this Kv channel subtype in the rat retina paralleled its role in the regulation of apoptosis [24]. Correspondingly, HSPA5, which was one of the retinal protein partners regulated by the major prion protein (PRNP), was shown to be exclusively involved in the ER stress response canonical pathway in the present study. The PRNP, which is an upstream regulator identified to be only implicated in the regulation of retinal protein partners in our investigation, is a predominant neuroprotective factor in the central nervous system including the retina and thus, mediate anti-apoptotic signal transduction [61]. Previous studies have elegantly

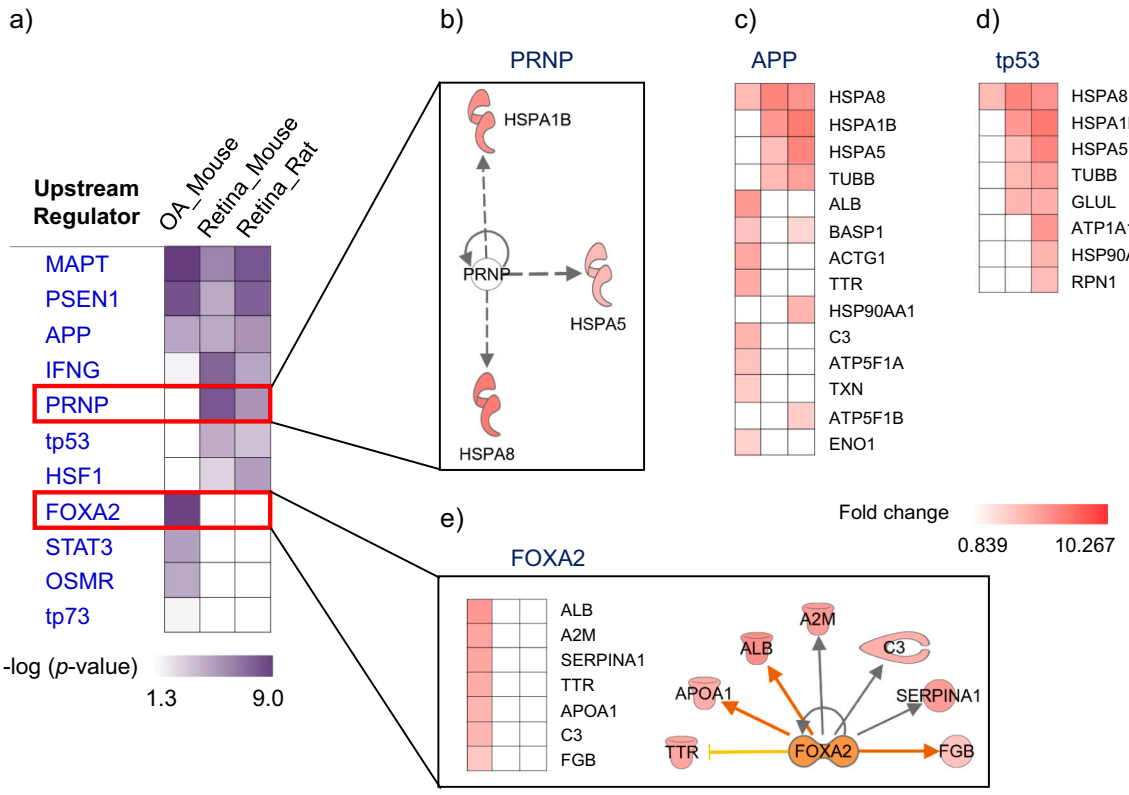

Fig. 9. Upstream regulators predicted to govern the downstream signalling of the Kv1.6 channel-associated protein clusters
(a) Elucidation of the top upstream regulators predicted to be significantly involved in the regulation of proteins in the ophthalmic artery and retina of different species with a significance threshold of -log (*p*-value) > 1.3. (b) Interaction network illustrates the regulation of one of predicted upstream regulators observed to experimentally affect only retinal proteins, PRNP. Heatmaps show the proteins regulated by (c) APP and (d) a transcription regulator, tp53, which were identified in all groups. (e) The regulation of ophthalmic arterial proteins by FOXA2 is depicted as heatmap and interaction network. The different shapes represent the functional classes of the proteins (*e.g.* enzyme, transcription regulator, transporter, *etc.*).

demonstrated that PRNP-encoded proteins have interactions with the auxiliary subunits of another Kv channel (Kv 4.2) and are involved in the direct modulation of certain ion channels [62,63]. Interestingly, the upregulation of PRNP modulated by the heat shock proteins was attributed to its protective role in cellular stress response; a regulatory pattern deemed similar to that of APP [48]. Collectively, these prodigious cell-protective activities of the Kv1.6 channel-interactome lend credence to our findings that cell survival mechanisms are activated in the retina of both species, while preserving the cell viability and vascular integrity in the ophthalmic artery.

Next, our work provides further evidence of several protein interactors that were identified exclusively in either the ophthalmic artery or the retina. Four protein partners of the Kv1.6 channel comprising HSPA1A, HSPA5, SLC25A5 and TUBB were identified only in the retinal tissue of both rodents. The SLC25A5 protein, better known as the adenine nucleotide translocase 2 (ANT2), is a protein in the class of active facilitative transporters, which is found most abundantly in the mitochondria of organs with high regenerative and proliferative properties such as the brain, liver and heart [64–67]. Strikingly, the majority of the SLC transporter proteins were shown to have a high degree of crosstalk and interaction with different ion channels including Kv channels; thus, earning the term 'chansporter' [68–70]. Consistent with the high metabolic demand of the retina [33], it is, therefore, not surprising that the most highly expressed transporter gene in this tissue with an essential role in the maintenance of cellular bioenergetics is the *SLC25A5* [71], which is in accordance with our current finding. This mitochondrial carrier protein plays a vital function by regulating the transport of ADP/ATP to provide energy to the cells [72]. Besides, this class of translocases is also known to particularly suppress apoptotic processes [73–75], a significant biological function, which was observed in our results. Another cluster of transporter proteins, which comprised A2M, ALB, APOA1 and TTR were found to be identified as Kv1.6 channel interacting partners exclusively in the ophthalmic artery. Interestingly, these proteins also encompassed the large majority of proteins regulated downstream by the transcription regulator, FOXA2. The latter belongs to the O subclass of the the forkhead family of transcription factors, which acts as transcriptional activator for genes encoding ALB and TTR in the liver [76]. Moreover, the expression of APOM, which is connected to APOA1, is directly regulated by FOXA2 in the hepatocytes [77]. Other Kv1.6 channel partners found to be exclusive to the retinal tissue and ophthalmic artery were the cytoskeleton proteins TUBB and ACTG1, respectively. Both proteins were also previously recognized to interact with another Kv channel subtype (Kv1.4) that was affinity-purified from the rat hippocampus [78]. Tubulin beta chain is a key neural-specific constituent of microtubules of the cytoskeleton, with a particularly high expression in the retinal ganglion cells owing to their neuronal origin [79,80], which was also shown to be involved in the organization of microtubules specifically attributed to the retina in our study. Tubulin protein was also shown to mediate regeneration of injured retina in zebrafish and influence the composition of cellular cytoarchitecture that affects cell survival ability [81,82].

It is also crucial to highlight here that p53 was one of the predicted upstream regulators with profound effect on many of the proteins identified to interact with the Kv1.6 channel in both retina and ophthalmic artery. This tumour suppressor transcription factor is ubiquitously expressed in all cell types and is usually latent until activated by an array of cellular insults, namely heat shock and oxidative stress [83]. Hence, p53 is a known 'client' of heat shock proteins as the former regulator plays specific roles in the modulation of the latter, which confers cell protective effects [84]. Albeit best known for its role as an

oncogene underlying cell arrest and apoptosis, there are accumulating evidence that p53 also possesses fundamental roles in lowering reactive oxygen species under normal physiological condition [83]. Accordingly, p53 is shown to be functionally relevant in oxidative stress-mediated cellular demise in the retinal ganglion cells [85]. In addition, this transcription factor is endowed with a novel role in protecting the vascular smooth muscle cells against apoptosis [86]. Taken together, the panoply of protein functions and their inter-connection to various cell signalling pathways and upstream regulators hint at the emergence of a broad paradigm in the modulatory influence of the Kv1.6 channel in major ocular vascular beds. The main limitation of this study is that further functional relevance of the various Kv1.6 channel-interacting proteins identified remains to be investigated in both ocular tissues, which is envisaged to be a topic for future investigation.

5. Conclusions

In conclusion, this is the first study that successfully enriched and identified the elusive Kv1.6 channel in ocular tissues using an optimized AP-MS approach, which is an important benchmark for future endeavours to further explore the functionality of this channel subtype. Importantly, this investigation has dissected the common interaction partners in the retina of two commonly used animal models in eye research, which is envisioned to be an advantageous basis for future studies systematically investigating possible functions of these newly identified Kv1.6 channel interacting proteins in retinopathies and neurodegenerative diseases. Finally, with our interest shifting from a tissue-centric view to a broader network-based approach, the mapping of ion channel proteomes in ocular tissues of different experimental animal models offers a new perspective on how the regulation of Kv1.6 channel can be tailored to study the (patho)physiology of eye diseases.

Supplementary data to this article can be found online at https://doi.org/10.1016/j.ijbiomac.2023.128464.

CRediT authorship contribution statement

NPe: Conceptualization, Resources, Investigation, Data curation, Formal analysis, Methodology, Writing - review and editing. HY: Investigation, Data curation, Formal analysis, Methodology, Writing - review and editing. KD: Formal analysis, Methodology, Writing - review and editing. KR: Resources, Methodology, Writing - review and editing. FHG: Resources, Writing - review and editing. NPf: Resources, Writing - review and editing. CM: Conceptualization, Project administration, Funding acquisition, Resources, Data curation, Supervision, Formal analysis, Investigation, Methodology, Writing-original draft, Writing-review and editing.

Funding

This work was supported by a grant from the German Research Foundation (DFG) (grant number: MA 8006/1-1) awarded to Caroline Manicam. The funders had no role in the study design, data collection and interpretation, or the decision to submit the work for publication.

Declaration of competing interest

None.

Data availability

All data generated and analysed in this study are included in the published article and its Supplementary Material Files.

Acknowledgements

Natarajan Perumal is supported by a DFG grant (PE 2531/4-1). The authors acknowledge the resources (IPA software) provided by the Institute of Medical Biostatistics, Epidemiology and Informatics (IMBEI) Core Facility of the University Medical Center Mainz.

References

[1] O. Nekrasova, A. Volyntseva, K. Kudryashova, V. Novoseletsky, E. Lyapina, A. Illarionova, S. Yakimov, Y.V. Korolkova, K. Shaitan, M. Kirpichnikov, Complexes of peptide blockers with Kv1. 6 pore domain: molecular modeling and studies with KcsA-Kv1. 6 channel, J. Neuroimmune Pharmacol. 12 (2) (2017) 260–276.
[2] I. Szabò, M. Zoratti, E. Gulbins, Contribution of voltage-gated potassium channels to the regulation of apoptosis, FEBS Lett. 584 (10) (2010) 2049–2056.
[3] B.D. Clark, E.M. Goldberg, B. Rudy, Electrogenic tuning of the axon initial segment, Neuroscientist 15 (6) (2009) 651–668.
[4] H. Kuba, R. Yamada, G. Ishiguro, R. Adachi, Redistribution of Kv1 and Kv7 enhances neuronal excitability during structural axon initial segment plasticity, Nat. Commun. 6 (2015) 8815.
[5] G. Yellen, The voltage-gated potassium channels and their relatives, Nature 419 (6902) (2002) 35–42.
[6] D.D. Bushart, A.J. Zalon, H. Zhang, L.M. Morrison, Y. Guan, H.L. Paulson, V. G. Shakkottai, H.S. McLoughlin, Antisense Oligonucleotide Therapy Targeted Against ATXN3 Improves Potassium Channel–Mediated Purkinje Neuron Dysfunction in Spinocerebellar Ataxia Type 3, Cerebellum 20 (1) (2021) 41–53.
[7] N.H. Shah, E. Aizenman, Voltage-gated potassium channels at the crossroads of neuronal function, ischemic tolerance, and neurodegeneration, Transl. Stroke Res. 5 (1) (2014) 38–58.
[8] M. Van Poucke, A.E. Vanhaesebrouck, L.J. Peelman, L. Van Ham, Experimental validation of in silico predicted KCNA1, KCNA2, KCNA6 and KCNQ2 genes for association studies of peripheral nerve hyperexcitability syndrome in Jack Russell terriers, Neuromuscul. Disord. 22 (6) (2012) 558–565.
[9] J. Zhu, J. Yan, W.B. Thornhill, The Kv1. 3 potassium channel is localized to the cis-Golgi and Kv1. 6 is localized to the endoplasmic reticulum in rat astrocytes, FEBS J. 281 (15) (2014) 3433–3445.
[10] S. Albarwani, L.T. Nemetz, J.A. Madden, A.A. Tobin, S.K. England, P.F. Pratt, N. J. Rusch, Voltage-gated K+ channels in rat small cerebral arteries: molecular identity of the functional channels, J. Physiol. 551 (3) (2003) 751–763.
[11] Y. Lu, S.T. Hanna, G. Tang, R. Wang, Contributions of Kv1. 2, Kv1. 5 and Kv2. 1 subunits to the native delayed rectifier K+ current in rat mesenteric artery smooth muscle cells, Life Sci. 71 (12) (2002) 1465–1473.
[12] C. Manicam, J. Staubitz, C. Brochhausen, F.H. Grus, N. Pfeiffer, A. Gericke, The gatekeepers in the mouse ophthalmic artery: endothelium-dependent mechanisms of cholinergic vasodilation, Sci. Rep. 6 (2016) 20322.
[13] A. Mori, R. Namekawa, K. Sakamoto, K. Ishii, T. Nakahara, 4-Aminopyridine, a voltage-gated K+ channel inhibitor, attenuates nitric oxide-mediated vasodilation of retinal arterioles in rats, Biol. Pharm. Bull. 43 (7) (2020) 1123–1127.
[14] Y. Nishijima, S. Cao, D.S. Chabowski, A. Korishettar, A. Ge, X. Zheng, R. Sparapani, D.D. Gutterman, D.X. Zhang, Contribution of Kv1. 5 channel to hydrogen peroxide–induced human arteriolar dilation and its modulation by coronary artery disease, Circ. Res. 120 (4) (2017) 658–669.
[15] V. Ohanyan, L. Yin, R. Bardakjian, C. Kolz, M. Enrick, T. Hakobyan, J. Kmetz, I. Bratz, J. Luli, M. Nagane, Requisite role of Kv1. 5 channels in coronary metabolic dilation, Circ. Res. 117 (7) (2015) 612–621.
[16] D.M. Kullmann, S.G. Waxman, Neurological channelopathies: new insights into disease mechanisms and ion channel function, J. Physiol. 588 (11) (2010) 1823–1827.
[17] R. Nelson, Potassium channels have a key role in neurodegeneration, The Lancet. Neurology 5 (4) (2006) 298–299.
[18] S. Stoilova-McPhie, S. Ali, F. Laezza, Protein-protein interactions as new targets for ion channel drug discovery, Austin Journal of Pharmacology and Therapeutics 1 (2) (2013) 5.
[19] M. Bachmann, W. Li, M.J. Edwards, S.A. Ahmad, S. Patel, I. Szabo, E. Gulbins, Voltage-gated potassium channels as regulators of cell death, Frontiers in Cell and Developmental Biology 8 (2020) 1571.
[20] E.A. Ko, W.S. Park, A.L. Firth, N. Kim, J.X.-J. Yuan, J. Han, Pathophysiology of voltage-gated K+ channels in vascular smooth muscle cells: modulation by protein kinases, Prog. Biophys. Mol. Biol. 103 (1) (2010) 95–101.
[21] H. Wulff, N.A. Castle, L.A. Pardo, Voltage-gated potassium channels as therapeutic targets, Nat. Rev. Drug Discov. 8 (12) (2009) 982–1001.
[22] D.J. Klumpp, D.B. Farber, C. Bowes, E.J. Song, L.H. Pinto, The potassium channel MBK1 (Kv1. 1) is expressed in the mouse retina, Cell. Mol. Neurobiol. 11 (6) (1991) 611–622.
[23] S. McFarlane, N.S. Pollock, A role for voltage-gated potassium channels in the outgrowth of retinal axons in the developing visual system, J. Neurosci. 20 (3) (2000) 1020–1029.
[24] K.M. Golla, T.R. Raju, S. Chatterji, Brain derived neurotrophic factor and superior collicular extract regulate the expression of the 1.6 subfamily of voltage-gated potassium channels in the developing rat retina in vitro, Journal of Ophthalmic & Vision Research 7 (2) (2012) 139–147.
[25] M. Höltje, I. Brunk, J. Grosse, E. Beyer, R. Veh, M. Bergmann, G. Grosse, G. Ahnert-Hilger, Differential distribution of voltage-gated potassium channels Kv 1.1–Kv1. 6 in the rat retina during development, J. Neurosci. Res. 85 (1) (2007) 19–33.
[26] L. De Groef, M. Cordeiro, M. Cordeiro, Is the eye an extension of the brain in CNS disease?, Journal of Ocular Pharmacology and Therapeutics 34(1–2) 129–133.

[27] A. London, I. Benhar, M. Schwartz, The retina as a window to the brain-from eye research to CNS disorders, Nat. Rev. Neurol. 9 (1) (2013) 44–53.
[28] V. Salpietro, V. Galassi Deforie, S. Efthymiou, E. O'Connor, A. Marcé-Grau, R. Maroofian, P. Striano, F. Zara, M.M. Morrow, S.S. Group, De novo KCNA6 variants with attenuated KV 1.6 channel deactivation in patients with epilepsy, Epilepsia 64 (2) (2023) 443–455.
[29] R. Gunasekaran, R.S. Narayani, K. Vijayalakshmi, P.A. Alladi, K. Shobha, A. Nalini, T. Sathyaprabha, T. Raju, Exposure to cerebrospinal fluid of sporadic amyotrophic lateral sclerosis patients alters Nav1. 6 and Kv1. 6 channel expression in rat spinal motor neurons, Brain Res. 1255 (2009) 170–179.
[30] Z.-P. Liu, L. Chen, Proteome-wide prediction of protein-protein interactions from high-throughput data, Protein Cell 3 (7) (2012) 508–520.
[31] B. Kim, R. Araujo, M. Howard, R. Magni, L.A. Liotta, A. Luchini, Affinity enrichment for mass spectrometry: improving the yield of low abundance biomarkers, Expert Rev. Proteomics 15 (4) (2018) 353–366.
[32] N. Perumal, A. Herfurth, N. Pfeiffer, C. Manicam, Short-term Omega-3 supplementation modulates novel neurovascular and fatty acid metabolic proteome changes in the retina and ophthalmic artery of mice with targeted *Cyp2c44* gene deletion, Cells 11 (21) (2022) 3494.
[33] N. Perumal, L. Straßburger, D.P. Herzog, M.B. Müller, N. Pfeiffer, F.H. Grus, C. Manicam, Bioenergetic shift and actin cytoskeleton remodelling as acute vascular adaptive mechanisms to angiotensin II in murine retina and ophthalmic artery, Redox Biol. 34 (2020), 101597.
[34] J. Han, M. Zhang, S. Froese, F.F. Dai, M. Robitaille, A. Bhattacharjee, X. Huang, W. Jia, S. Angers, M.B. Wheeler, The identification of novel protein-protein interactions in liver that affect glucagon receptor activity, PloS One 10 (6) (2015), e0129226.
[35] K. Meyer, M. Selbach, Quantitative affinity purification mass spectrometry: a versatile technology to study protein–protein interactions, Front. Genet. 6 (2015) 237.
[36] N.C. Wildburger, S.R. Ali, W.-C.J. Hsu, A.S. Shavkunov, M.N. Nenov, C.F. Lichti, R. D. LeDuc, E. Mostovenko, N.I. Panova-Elektronova, M.R. Emmett, Quantitative proteomics reveals protein–protein interactions with fibroblast growth factor 12 as a component of the voltage-gated sodium channel 1.2 (nav1. 2) macromolecular complex in mammalian brain, Mol. Cell. Proteomics 14 (5) (2015) 1288–1300.
[37] N. Perumal, L. Straßburger, C. Schmelter, A. Gericke, N. Pfeiffer, F.H. Grus, C. Manicam, Sample preparation for mass-spectrometry-based proteomics analysis of ocular microvessels, JoVE (Journal of Visualized Experiments) 144 (2019) 1–11.
[38] J. Cox, M. Mann, MaxQuant enables high peptide identification rates, individualized ppb-range mass accuracies and proteome-wide protein quantification, Nat. Biotechnol. 26 (12) (2008) 1367–1372.
[39] J. Cox, N. Neuhauser, A. Michalski, R.A. Scheltema, J.V. Olsen, M. Mann, Andromeda: a peptide search engine integrated into the MaxQuant environment, J. Proteome Res. 10 (4) (2011) 1794–1805.
[40] S. Tyanova, T. Temu, J. Cox, The MaxQuant computational platform for mass spectrometry-based shotgun proteomics, Nat. Protoc. 11 (12) (2016) 2301–2319.
[41] A. Krämer, J. Green, J. Pollard Jr., S. Tugendreich, Causal analysis approaches in ingenuity pathway analysis, Bioinformatics 30 (4) (2014) 523–530.
[42] P.R. Dores-Silva, D.M. Cauvi, A.L. Coto, N.S. Silva, J.C. Borges, A. De Maio, Human heat shock cognate protein (HSC70/HSPA8) interacts with negatively charged phospholipids by a different mechanism than other HSP70s and brings HSP90 into membranes, Cell Stress and Chaperones 26 (4) (2021) 671–684.
[43] M. Iftinca, R. Flynn, L. Basso, H. Melo, R. Aboushousha, L. Taylor, C. Altier, The stress protein heat shock cognate 70 (Hsc70) inhibits the transient receptor potential Vanilloid type 1 (TRPV1) channel, Mol. Pain 12 (2016), 1744806916663945.
[44] S.C. Grifoni, S.E. McKey, H.A. Drummond, Hsc70 regulates cell surface ASIC2 expression and vascular smooth muscle cell migration, Am. J. Phys. Heart Circ. Phys. 294 (5) (2008) H2022–H2030.
[45] F. Stricher, C. Macri, M. Ruff, S. Muller, HSPA8/HSC70 chaperone protein: structure, function, and chemical targeting, Autophagy 9 (12) (2013) 1937–1954.
[46] M. Bianchi, R. Crinelli, V. Arbore, M. Magnani, Induction of ubiquitin C (UBC) gene transcription is mediated by HSF 1: role of proteotoxic and oxidative stress, FEBS Open Bio 8 (9) (2018) 1471–1485.
[47] R. Crinelli, M. Bianchi, L. Radici, E. Carloni, E. Giacomini, M. Magnani, Molecular dissection of the human ubiquitin C promoter reveals heat shock element architectures with activating and repressive functions, PloS One 10 (8) (2015), e0136882.
[48] W.-C. Shyu, M.-C. Kao, W.-Y. Chou, Y.-D. Hsu, B.-W. Soong, Heat shock modulates prion protein expression in human NT-2 cells, Neuroreport 11 (4) (2000) 771–774.
[49] E.M. Knight, H.H. Ruiz, S.H. Kim, J.C. Harte, W. Hsieh, C. Glabe, W.L. Klein, A. D. Attie, C. Buettner, M.E. Ehrlich, Unexpected partial correction of metabolic and behavioral phenotypes of Alzheimer's APP/PSEN1 mice by gene targeting of diabetes/Alzheimer's-related Sorcs1, Acta Neuropathol. Commun. 4 (2016) 16.
[50] X. Li, J. Long, T. He, R. Belshaw, J. Scott, Integrated genomic approaches identify major pathways and upstream regulators in late onset Alzheimer's disease, Sci. Rep. 5 (2015) 12393.
[51] M.A.G. Sosa, R. De Gasperi, P.R. Hof, G.A. Elder, Fibroblast growth factor rescues brain endothelial cells lacking presenilin 1 from apoptotic cell death following serum starvation, Sci. Rep. 6 (2016) 30267.
[52] A. Cojocaru, E. Burada, A.-T. Bălșeanu, A.-F. Deftu, B. Cătălin, A. Popa-Wagner, E. Osiac, Roles of microglial Ion Channel in neurodegenerative diseases, J. Clin. Med. 10 (6) (2021) 1239.
[53] S. Rangaraju, M. Gearing, L.-W. Jin, A. Levey, Potassium channel Kv1. 3 is highly expressed by microglia in human Alzheimer's disease, J. Alzheimers Dis. 44 (3) (2015) 797–808.
[54] E. Chavakis, S. Dimmeler, Regulation of endothelial cell survival and apoptosis during angiogenesis, Arterioscler. Thromb. Vasc. Biol. 22 (6) (2002) 887–893.
[55] R. De Gasperi, M.A.G. Sosa, G.A. Elder, Presenilin-1 regulates the constitutive turnover of the fibronectin matrix in endothelial cells, BMC Biochem. 13 (2012) 28.
[56] G. Deng, C.J. Pike, C.W. Cotman, Alzheimer-associated presenilin-2 confers increased sensitivity to poptosis in PC12 cells, FEBS Lett. 397 (1) (1996) 50–54.
[57] Q. Guo, B.L. Sopher, K. Furukawa, D.G. Pham, N. Robinson, G.M. Martin, M. P. Mattson, Alzheimer's presenilin mutation sensitizes neural cells to apoptosis induced by trophic factor withdrawal and amyloid β-peptide: involvement of calcium and oxyradicals, J. Neurosci. 17 (11) (1997) 4212–4222.
[58] M.P. Mattson, Q. Guo, K. Furukawa, W.A. Pedersen, Presenilins, the endoplasmic reticulum, and neuronal apoptosis in Alzheimer's disease, J. Neurochem. 70 (1) (1998) 1–14.
[59] B. Wolozin, P. Alexander, J. Palacino, Regulation of apoptosis by presenilin 1, Neurobiol. Aging 19 (1 Suppl) (1998) S23–S27.
[60] M.-J. Gething, Role and regulation of the ER chaperone BiP, Semin. Cell Dev. Biol. 10 (5) (1999) 465–472.
[61] J. Herms, T. Tings, S. Gall, A. Madlung, A. Giese, H. Siebert, P. Schürmann, O. Windl, N. Brose, H. Kretzschmar, Evidence of presynaptic location and function of the prion protein, J. Neurosci. 19 (20) (1999) 8866–8875.
[62] R.C. Mercer, L. Ma, J.C. Watts, R. Strome, S. Wohlgemuth, J. Yang, N.R. Cashman, M.B. Coulthart, G. Schmitt-Ulms, J.H. Jhamandas, The prion protein modulates A-type K+ currents mediated by Kv4. 2 complexes through dipeptidyl aminopeptidase-like protein 6, J. Biol. Chem. 288 (52) (2013) 37241–37255.
[63] M.-A. Wulf, A. Senatore, A. Aguzzi, The biological function of the cellular prion protein: an update, BMC Biol. 15 (1) (2017) 34.
[64] A.-S. Belzacq, H.L. Vieira, G. Kroemer, C. Brenner, The adenine nucleotide translocator in apoptosis, Biochimie 84 (2–3) (2002) 167–176.
[65] V. Dolce, P. Scarcia, D. Iacopetta, F. Palmieri, A fourth ADP/ATP carrier isoform in man: identification, bacterial expression, functional characterization and tissue distribution, FEBS Lett. 579 (3) (2005) 633–637.
[66] Y. Liu, X.J. Chen, Adenine nucleotide translocase, mitochondrial stress, and degenerative cell death, Oxid. Med. Cell. Longev. 2013 (2013), 146860.
[67] Y. Zhang, Y. Zhang, K. Sun, Z. Meng, L. Chen, The SLC transporter in nutrient and metabolic sensing, regulation, and drug development, J. Mol. Cell Biol. 11 (1) (2019) 1–13.
[68] V.A. Baronas, R.Y. Yang, L.C. Morales, S. Sipione, H.T. Kurata, Slc7a5 regulates Kv1. 2 channels and modifies functional outcomes of epilepsy-linked channel mutations, Nature Communications 9 (1) (2018) 4417.
[69] D.L. Neverisky, G.W. Abbott, Ion channel–transporter interactions, Crit. Rev. Biochem. Mol. Biol. 51 (4) (2016) 257–267.
[70] L. Rochette, A. Meloux, M. Zeller, G. Malka, Y. Cottin, C. Vergely, Mitochondrial SLC25 carriers: novel targets for cancer therapy, Molecules 25 (10) (2020) 2417.
[71] A. Dahlin, E. Geier, S.L. Stocker, C.D. Cropp, E. Grigorenko, M. Bloomer, J. Siegenthaler, L. Xu, A.S. Basile, D.D. Tang-Liu, Gene expression profiling of transporters in the solute carrier and ATP-binding cassette superfamilies in human eye substructures, Mol. Pharm. 10 (2) (2013) 650–663.
[72] B. Clémençon, M. Babot, V. Trézéguet, The mitochondrial ADP/ATP carrier (SLC25 family): pathological implications of its dysfunction, Mol. Aspects Med. 34 (2–3) (2013) 485–493.
[73] A. Chevrollier, D. Loiseau, P. Reynier, G. Stepien, Adenine nucleotide translocase 2 is a key mitochondrial protein in cancer metabolism, Biochimica et Biophysica Acta (BBA)-Bioenergetics 1807 (6) (2011) 562–567.
[74] W. Malorni, M. Farrace, P. Matarrese, A. Tinari, L. Ciarlo, P. Mousavi-Shafaei, M. D'eletto, G. Di Giacomo, G. Melino, L. Palmieri, The adenine nucleotide translocator 1 acts as a type 2 transglutaminase substrate: implications for mitochondrial-dependent apoptosis, Cell Death & Differentiation 16 (11) (2009) 1480–1492.
[75] P. Singh, S. Suman, S. Chandna, T.K. Das, Possible role of amyloid-beta, adenine nucleotide translocase and cyclophilin-D interaction in mitochondrial dysfunction of Alzheimer's disease, Bioinformation 3 (10) (2009) 440–445.
[76] P. Madeddu, FoxA2 hunting research identifies the early trail of mesenchymal differentiation, Stem Cell Res Ther 4 (2) (2013) 40.
[77] Y.-W. Hu, L. Zheng, Q. Wang, T.-Y. Zhong, X. Yu, J. Bao, N.-N. Cao, B. Li, B. Si-Tu, Vascular endothelial growth factor downregulates apolipoprotein M expression by inhibiting Foxa2 in a Nur77-dependent manner, Rejuvenation Res. 15 (4) (2012) 423–434.
[78] C. Xie, H. Su, T. Guo, Y. Yan, X. Peng, R. Cao, Y. Wang, P. Chen, X. Wang, S. Liang, Synaptotagmin I delays the fast inactivation of Kv1. 4 channel through interaction with its N-terminus, Molecular Brain 7 (2014) 4.
[79] M. Bosch Grau, C. Masson, S. Gadadhar, C. Rocha, O. Tort, P. Marques Sousa, S. Vacher, I. Bieche, C. Janke, Alterations in the balance of tubulin glycylation and glutamylation in photoreceptors leads to retinal degeneration, J. Cell Sci. 130 (5) (2017) 938–949.
[80] S.-M. Jiang, L.-P. Zeng, J.-H. Zeng, L. Tang, X.-M. Chen, X. Wei, β-III-tubulin: a reliable marker for retinal ganglion cell labeling in experimental models of glaucoma, Int. J. Ophthalmol. 8 (4) (2015) 643–652.
[81] B.V. Fausett, D. Goldman, A role for α1 tubulin-expressing Müller glia in regeneration of the injured zebrafish retina, J. Neurosci. 26 (23) (2006) 6303–6313.
[82] R.K. Sharma, P.A. Netland, Early born lineage of retinal neurons express class III β-tubulin isotype, Brain Res. 1176 (2007) 11–17.
[83] J.J. Salazar, R. Gallego-Pinazo, R. de Hoz, M.D. Pinazo-Durán, B. Rojas, A. I. Ramírez, M. Serrano, J.M. Ramírez, "Super p53" mice display retinal astroglial changes, PloS One 8 (6) (2013), e65446.

[84] X. Han, F. Wang, W. Yao, H. Xing, D. Weng, X. Song, G. Chen, L. Xi, T. Zhu, J. Zhou, Heat shock proteins and p53 play a critical role in K+ channel-mediated tumor cell proliferation and apoptosis, Apoptosis 12 (10) (2007) 1837–1846.
[85] L. Vuong, S.M. Conley, M.R. Al-Ubaidi, Expression and role of p53 in the retina, Invest. Ophthalmol. Vis. Sci. 53 (3) (2012) 1362–1371.
[86] J. Mercer, N. Figg, V. Stoneman, D. Braganza, M.R. Bennett, Endogenous p53 protects vascular smooth muscle cells from apoptosis and reduces atherosclerosis in ApoE knockout mice, Circ. Res. 96 (6) (2005) 667–674.